Hindawi Publishing Corporation
International Journal of Antennas and Propagation
Volume 2015, Article ID 797352, 21 pages
http://dx.doi.org/10.1155/2015/797352

Review Article

Aspects of the Subarrayed Array Processing for the Phased Array Radar

Hang Hu

School of Electronics and Information Engineering, Harbin Institute of Technology, Harbin 150001, China

Correspondence should be addressed to Hang Hu; huhang@hit.edu.cn

Received 20 June 2014; Revised 25 November 2014; Accepted 25 November 2014

Academic Editor: Michelangelo Villano

This paper gives an overview on the research status, developments, and achievements of subarrayed array processing for the multifunction phased array radar. We address some issues concerning subarrayed adaptive beamforming, subarrayed fast-time space-time adaptive processing, subarray-based sidelobe reduction of sum and difference beam, subarrayed adapted monopulse, subarrayed superresolution direction finding, subarray configuration optimization in ECCM (electronic counter-countermeasure), and subarrayed array processing for MIMO-PAR. In this review, several viewpoints relevant to subarrayed array processing are pointed out and the achieved results are demonstrated by numerical examples.

1. Introduction

PAR (phased array radar) and especially MFPAR (multifunction PAR) often adopt a subarrayed antenna array. SASP (subarrayed array signal processing) is one of the key technologies in modern PARs and plays a key role in the MFPAR.

In this paper we consider the modern MFPAR with an element number of the order of 1000 (assume that the subarrays are compact and nonoverlapping) and with amplitude tapering (e.g., Taylor weighting) applied at the elements for low sidelobes. And the steering into the look direction is done by phase shifting at the elements. Assume the MFPAR with many modes of operation (e.g., search, track, and high resolution) and all processing to be performed digitally with the subarray outputs.

The key technologies and issues of SASP include subarray weighting for quiescent pattern synthesis and PSL (peak sidelobe) reduction, subarrayed adaptive interference suppression with subarrayed ABF (adaptive beamforming) or ASLB (adaptive sidelobe blanking), subarrayed adaptive detection, subarrayed parameter estimation, for instance, adaptive monopulse and superresolution direction finding, optimization of subarray configuration, and an expansion of the SASP, that is, application in MIMO- (multiple-input multiple-output-) PAR, and so forth.

Nickel is the pioneer and trailblazer in the field of the SASP. Since the 1990s, he has firstly systematically performed a series of thorough researches which theoretically and technically lay the solid foundation of the SASP. His research achievements represent the development level of SASP technology [1]. Nickel's reserches covered all kinds of key technologies in SASP, including subarray weighting for PSL reduction [2], adaptive interference suppression (ABF and ASLB) [3–5], slow- and fast-time STAP (space-time adaptive processing) [6–9], influence of channel errors [6, 10], multiple BF (beam forming) with low sidelobes [11], adaptive detection [5, 8], adaptive monopulse [9, 12–18], superresolution [6, 19], adaptive tracking [20–24], and design of optimum subarrays [2]. The achievements have formed a complete theoretical system and framework of the SASP.

Similarly, Farina with different coauthors has given creative and pioneering contributions to the following aspects, including subarrayed weighting for SLC [25, 26], subarrayed adaptation and superresolution [25–27], and subarray optimization [25, 28]. Lombardo and his co-authors contributed great achievements to subarrayed adaptive processing and pattern control [29, 30], SASP for thinned arrays [31, 32], while Massa et al. contributed in the fields of subarrayed weighting, synthesis of sum and difference patterns for monopulse [33–36]; Liao et al. in the field of subarrayed

ABF, subarrayed STAP and subarray architectures [23, 37, 38]; Wang et al. in the field of subarrayed STAP and subarray configuration [39–42]; Klemm in the field of the design of the subarray configuration for STAP [43], and so forth.

SASP possesses a good application prospect for millimeter wave PAR seeker, airborne multifunction radar, and space-borne early-warning radar. A famous and outstanding example is the tri-national X-band AMSAR project for a future European airborne radar [7].

This paper summarizes the research achievements in the field of SASP including the study results of the author. The relevant issues focus on subarrayed ABF, subarrayed fast-time STAP, subarrayed PSL reduction for sum and difference beam, PSL reduction for subarrayed beam scanning, subarrayed adapted monopulse, subarrayed superresolution direction finding, subarray optimization for ECCM (electronic counter-countermeasure), and the SASP for MIMO-PAR.

In this review, viewpoints and innovative ways are presented which are relevant to the SASP. For the proposed algorithms we give examples.

2. Subarrayed ABF

In this section we investigate subarrayed ABF and adaptive interference suppression. Actually, the adaptive weighting is implemented at subarray level. The subarrayed ABF has three configurations, that is, DSW (direct subarray weighting), SLC (sidelobe canceller), and GSLC (generalized SLC) types [16]. The three concepts are shown in Figure 1.

The limitation of DSW configuration is that it requires an estimation of the interference-plus-noise covariance matrix. The matrix is necessary for the estimation of adaptive weights. The limitation of the subarrayed SLC configuration is that equipment with auxiliary antennas and auxiliary channels is required, as indicated in Figure 1(b). The advantage of subarrayed GSLC is less equipment complexity compared with subarrayed SLC, because the auxiliary channels need not single elements but may be generated from the array itself by subarrays as indicated in Figure 1(c). Furthermore, compared with the DSW, the SLC and the GSLC do not need an estimation of interference plus noise covariance matrix (since the jammer signal can be subtracted from the main channel by the weighted sum of auxiliary channels outputs, Figures 1(b) and 1(c)).

This section is devoted to the DSW and GSLC configurations.

2.1. DSW Type Subarrayed ABF

2.1.1. Subarrayed Optimum ABF. First consider the subarrayed optimum BF (optimum adaptive filter [30]), in which weight vector $\mathbf{w}$ is obtained by direct weighting of the subarray outputs. From the likelihood ratio test criterion, the probability of detection is maximized if the weight vector maximizes the SINR for a desired signal [1]. As a consequence, $\mathbf{w} = \mu\widehat{\mathbf{R}}^{-1}\mathbf{a}(\theta_0,\varphi_0)$, where $\widehat{\mathbf{R}}$ is an estimate of the interference-plus-noise covariance matrix at subarray level, $\mathbf{a}(\theta_0, \varphi_0)$ denotes the steering vector at look direction, and μ is a nonzero constant. The maximum likelihood estimate of covariance matrix is $\widehat{\mathbf{R}}_{\mathrm{SMI}}$, that is, taking the average over the subarray output data [1]. This method is also called the subarrayed SMI (sample matrix inverse).

2.1.2. Improved Versions of Subarrayed SMI. The shortcoming of the subarrayed SMI is that the sidelobe level of adapted pattern is increased remarkably compared with quiescent pattern with tapering weighting due to subarrayed weighting (assuming the subarray transformation matrix $\mathbf{T}$ is not normalized), especially in the case of the absence of the jamming.

Suppose that we have an array with N elements divided into L subarrays. $\mathbf{T}$ can be written by

$$\mathbf{T} = \mathbf{\Phi}\mathbf{W}\mathbf{T}_0 \tag{1}$$

with $\mathbf{\Phi} = \mathrm{diag}[\boldsymbol{\varphi}_n(\theta_0, \varphi_0)]_{n=0,\ldots,N-1}$; hereinto $\boldsymbol{\varphi}_n(\theta_0, \varphi_0)$ represents the effect of the phase shifting of the nth element; $\mathbf{W} = \mathrm{diag}(w_n)_{n=0,\ldots,N-1}$, where w_n is the weight of the nth element used to suppress sidelobe level of sum pattern. $\mathbf{T}_0$ is the $N\times L$-dimensional subarray forming matrix, in all the elements of the lth $(l = 0, \ldots, L-1)$ column, only if the element belongs to lth subarray the element value is 1; otherwise it is 0.

On the other hand, the subarrayed SMI has only asymptotically a good performance. In practice, we have to draw on a variety of techniques to provide robust performance in the case of small sample size. The improved versions of subarrayed SMI comprise the subarrayed LSMI (load sample matrix inversion), the subarrayed LMI (lean matrix inversion), and so forth. The subarrayed LSMI and the subarrayed LMI are the extensions of LSMI [44] and LMI [45], respectively.

2.1.3. Quiescent Pattern Control Approaches. Quiescent pattern control approaches are another kind of the improved versions of subarrayed optimum ABF. The approaches preserve the desired quiescent pattern in the absence of jammer. Therefore, they make system automatically converge to the nonadapting mode. Thus the conversion problem between the two working modes of the subarrayed ABF is resolved [30]. Furthermore, quiescent pattern control approaches improve the PSL remarkably compared with subarrayed optimum ABF in the presence of jammers [46].

The pattern control approaches include normalization method, MOD (mismatched optimum detector), and SSP (subspace projection). Therein, the starting point of the normalization method [2, 25, 29, 30] is the amplitude taper combined with the different number of elements for each subarray, which implies the receiver noise level is different at the subarray output. The subarrayed ABF tries to find a weight giving equal noise power in all subarrays and cancels the low sidelobe taper; that is, the adapted weight tends to be the vector with uniform tapering. Then we can adopt normalization method to overcome this effect, that is, to normalize the outputs of subarrays before adaptation so that the noise powers at the subarray outputs are equal.

The MOD [29] introduces a mismatched steering vector, so that the adaptive beamformer detects such a mismatched target and yields quiescent pattern in the absence of jammers.

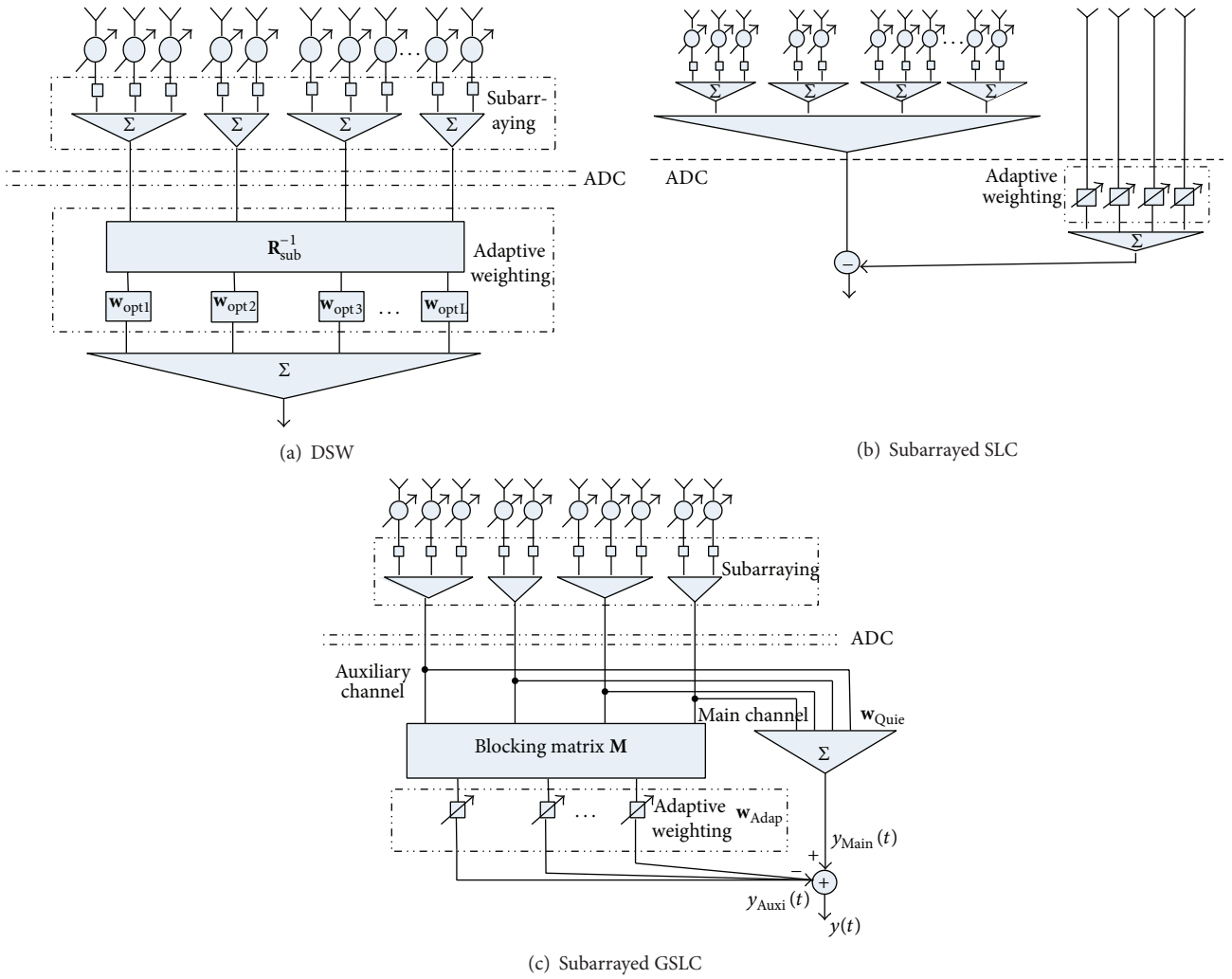

Figure 1: Configurations of subarrayed ABF.

The mismatched steering vector is written by $\mathbf{a}'(\theta_0, \varphi_0) = \mathbf{R}_{\text{SMI}}{}^{(0)}\mathbf{q}$, the superscript (0) indicates the absence of jammer. Assume that $\mathbf{q}$ denotes the quiescent control vector, namely, the $L \times 1$ column vector, in which all the elements are equally 1. As a consequence, in the case of absence of jammer, the adaptive weights are $\mathbf{w}^{(0)} = \mu\mathbf{q}$. Thereby, the quiescent pattern control is achieved. Compared with the normalization method, the MOD does not need preprocessing and a recovery operator; therefore the computational cost is reduced remarkably.

The SSP [29] consists of the following steps: (1) obtaining the first subspace and getting the quiescent patterns by using $\mathbf{q}$ to combine subarray outputs, (2) finding the subspace which distorts the quiescent pattern and discarding it, and (3) making the optimum interference suppression in the remaining $L - 2$ dimensional space which does not impact the quiescent pattern.

Table 1 presents the contrast of the performance for the quiescent pattern control approaches, obviously, in which the MOD is suitable for the overlapped subarrays and has small computational burden compared with other models.

2.1.4. The Approach Combining the Subarrayed Optimum ABF with the Quiescent Pattern Control [46]. Following we present an improvement of quiescent pattern control approaches. For the pattern control, the PSL reduction capability is at the cost of degradation of adaptation. This results in an output SINR loss. On the other hand, for the subarrayed optimum ABF, the anti-jamming capability is optimum. In order to compromise PSL and adaptation capability, we put forward the methods combining subarrayed optimum ABF and quiescent pattern control. The adaptive weight is

$$\mathbf{w}^{(\text{com})} = K_{\text{Opt}}\mathbf{w}_{\text{Opt}} + K_{\text{QPC}}\mathbf{w}_{\text{QPC}}, \tag{2}$$

where $\mathbf{w}_{\text{Opt}}$ and $\mathbf{w}_{\text{QPC}}$ denote the weights of the subarrayed optimum ABF and quiescent pattern control approach, respectively. And $K_{\text{Opt}} + K_{\text{QPC}} = 1.0$.

The combined method unifies subarrayed optimum ABF and quiescent pattern control, both of which are two extreme cases of the combined method. The combined method improves the flexibility of the PSL reduction for adaptive pattern and makes the trade-off between PSL and SINR according to real requirements. When we want to obtain

Table 1: Performance contrast of quiescent pattern control approaches.

	Suitability for overlapped subarrays	Computational burden
MOD	Suitable	Very small
Normalization method	Nonsuitable	Large
SSP	Suitable	Very heavy

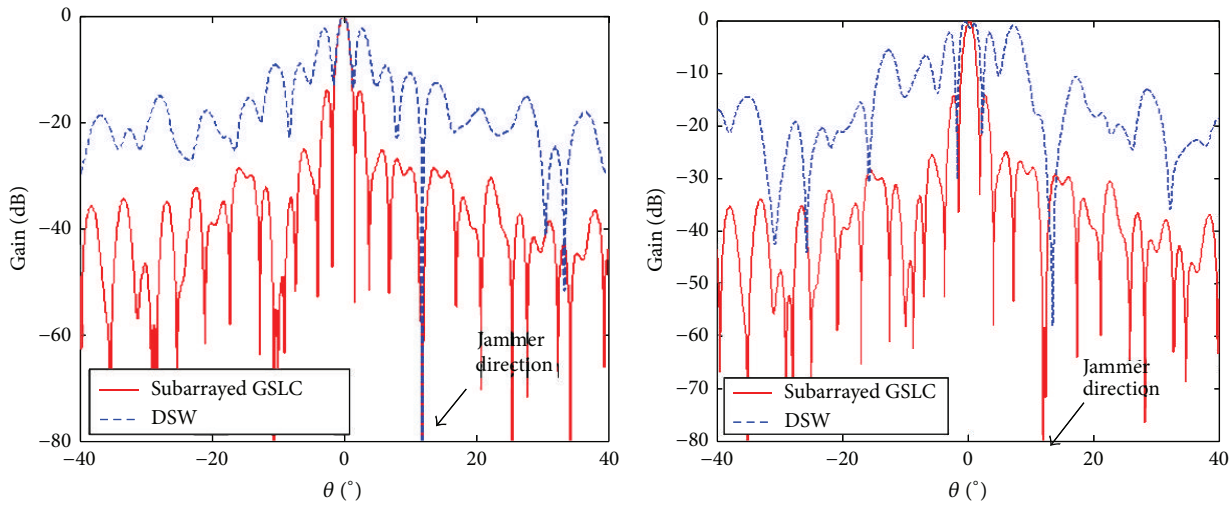

(a) Amplitude errors (b) Phase errors

Figure 2: Adaptive patterns with I/Q errors.

better PSL reduction capability, we can choose higher value of K_{QPC}; otherwise, we can set a higher value of K_{Opt} to reduce SINR loss. Through choosing appropriate parameters, combined method can reduce PSL effectively, and the achieved SINR is closely approximate to the SINR of subarrayed optimum ABF as well.

The above-mentioned quiescent pattern control method and the combining method can be extended into subarrayed fast-time STAP, as will be shown in Section 3.

2.2. GSLC-Based Subarrayed ABF. In the subarrayed GSLC, the blocking matrix in auxiliary channel (Figure 1(c)) is used for removing the desired signal component from this channel, in which simplest form is only difference operation of adjacent subarray outputs [47]. However, its blocking capability is poor. Consequently, residual signal component would be cancelled which leads to the degradation of output SINR. For this reason we introduce the Householder transform to determine the blocking matrix [48].

Let

$$\mathbf{e} = [1, 0, \ldots, 0]^T_{L\times 1},$$
$$\mathbf{p} = \frac{\mathbf{a}(\theta_0, \varphi_0) - \|\mathbf{a}(\theta_0, \varphi_0)\|_2 \mathbf{e}}{\|\mathbf{a}(\theta_0, \varphi_0) - \|\mathbf{a}(\theta_0, \varphi_0)\|_2 \mathbf{e}\|_2}, \tag{3}$$

where $\|\cdot\|_2$ is 2-norm. Then the Householder matrix is

$$\mathbf{H} = \mathbf{I} - 2\mathbf{p}\mathbf{p}^T, \tag{4}$$

of which the first column is $\mathbf{a}(\theta_0, \varphi_0)$ and the remaining $L-1$ ones are orthogonal to $\mathbf{a}(\theta_0, \varphi_0)$, respectively. Accordingly, $\mathbf{M}$ in Figure 1(c) is

$$\mathbf{M} = \mathbf{H}\begin{bmatrix} 0 & \cdots & 0 & 0 \\ 1 & \cdots & 0 & 0 \\ \vdots & \ddots & \vdots & \vdots \\ 0 & \cdots & 1 & 0 \\ 0 & \cdots & 0 & 1 \end{bmatrix}_{L\times(L-1)}. \tag{5}$$

The adaptive patterns and output SINR obtained by Householder transform-based GSLC are the same as that of the optimum ABF-based DSW [48]. On the other hand, the robustness of the subarrayed GSLC is much better than DSW. We assume a ULA (uniform linear array) comprising 92 elements is partitioned into 10 nonoverlapped subarrays. Then −40 dB Taylor weighting is applied. The jammer direction θ_j is 12°, JNR (jammer-to-noise ratio) is 35 dB, signal power p_s = 1, and the noise at element is AGWN (additional Gaussian white noise). Following we consider the errors at subarray level produced by the receivers which create the I- and Q-channels. Assume the amplitude errors obey the distribution of $N(0, 0.1)$ with the ideal error-free amplitude gain of the I- and Q-channel being 1 and a normalized parameter being 0.1, while phase errors obey the distribution of $N(0, 1)$ with the unit of degree. Figure 2 shows the adaptive patterns of the subarrayed GSLC with Householder transform. It is obvious that all respects such as the look direction, the beam shape,

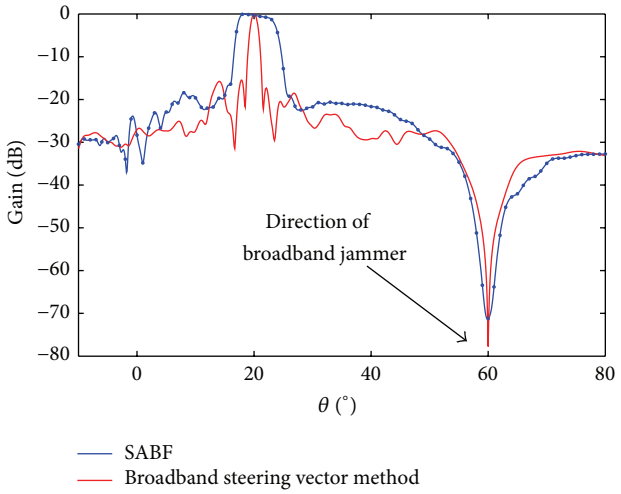

Figure 3: Adapted pattern obtained with subarrayed broadband ABF.

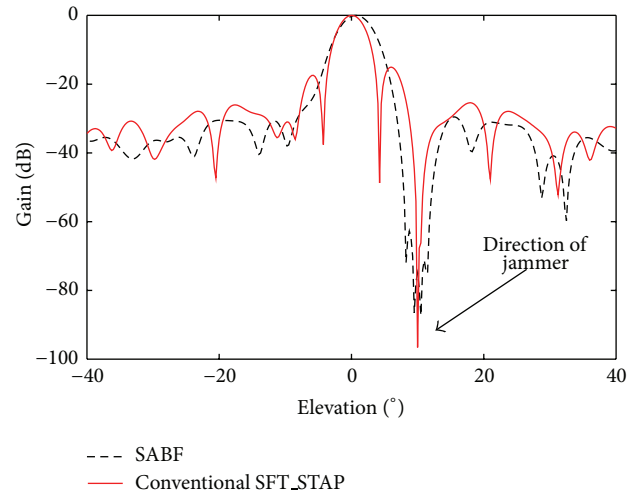

Figure 4: Adaptive patterns in the case of broadband jammer (cut patterns in azimuth plane).

the direction and depth of jammer notch, and the PSL are much better than those of optimum ABF-based DSW.

The subarrayed GSLC with Householder transform is valid no matter it is with amplitude errors or phase errors, which is insensitive to phase errors even.

2.3. The Subarrayed Broadband ABF. For the broadband array, additional time delays at subarray outputs are adopted in order to compensate phase difference of internal subarray of each frequency component. The look direction is controlled by subarray time-delay and phase shifter together for whole working bandwidth.

The adaptive weights of subarrayed broadband ABF can be obtained through broadband steering vector method. This method controls the look direction for each frequency of working bandwidth and realizes gain condition constraints, that is, makes the gain for each frequency to be equal. Assume bandwidth of all jammers is B and the power spectrum density obeys the uniform distribution in $[f_0 - B/2, f_0 + B/2]$; then the subarrayed steering vector is

$$\mathbf{a}(\theta,\varphi) = \int_{f_0-B/2}^{f_0+B/2} \mathbf{T}_D{}^H \mathbf{a}_{\text{ele}}(f,\theta,\varphi)\,\mathrm{d}f, \tag{6}$$

where $\mathbf{T}_D$ represents subarray transformation matrix with subarray time-delay effect; $\mathbf{a}_{\text{ele}}(f,\theta,\varphi) = [1,\ldots,e^{-j2\pi f\tau_n(\theta,\varphi)},\ldots,e^{-j2\pi f\tau_{N-1}(\theta,\varphi)}]^T$; hereinto $\tau_n(\theta,\varphi)$ is the time difference relative to reference element.

Assume that a ULA consisting of 99 elements is partitioned into 25 nonuniform subarrays; the relative bandwidth is $B/f_0 = 10\%$; element spacing is $\lambda_0/2$ (λ_0 is wavelength at f_0). And −40 dB Taylor weighting is applied. Let $\theta_0 = -60^\circ$ and $\theta_j = -20^\circ$. Figure 3 illustrates a resulting adapted pattern obtained with broadband steering vector method-based subarrayed broadband ABF [49]. It is drawn that the look direction and mainlobe shape of the adapted pattern is maintained, whereas the subarrayed ABF (SABF for short) has an obvious mainlobe broadening.

3. Subarrayed Fast-Time STAP

In the recent twenty years, extensive and thorough research on slow-time STAP used for clutter mitigation in airborne radar has been carried out [40, 43]. This paper only focuses on the fast-time STAP and this section is concerned with the subarrayed fast-time STAP.

In the presence of broadband jammers, subarrayed ABF would form broad adaptive nulls, which consumes spatial degrees of freedom and distorts the beam shape as indicated in Figure 3. For this reason, we should adopt subarrayed fast-time STAP [6].

The subarrayed ABF methods presented in Section 2 can be applied analogously in the space-time domain. The subarrayed fast-time STAP includes three kinds of structures, namely, DSW, SLC, and GSLC type. For example, for the DSW type subarrayed fast-time STAP, delay-weighting network is used at each subarray output (the number of delays is equal for each subarray). The delays aim to provide phase compensation for each frequency component in bandwidth. Meanwhile, adaptive weights are applied at all delay outputs of each subarray to achieve broadband interference suppression.

To give an example, suppose a UPA (uniform planar array) with 32×34 elements, and in both x and y directions the element spacing is $\lambda_0/2$. A −40 dB Taylor weighting is applied in both x and y directions. Array is partitioned into 6×6 nonuniform subarrays, each of which is a rectangle planar array. Suppose $B/f_0 = 10\%$ for the jammer. We set the number of delay $K = 4$. Figure 4 plots patterns in the presence of SLJ (sidelobe jamming), where SFT_STAP is an abbreviation of subarrayed fast-time STAP. By comparing two approaches, we see a narrow null of subarrayed fast-time STAP, while subarrayed ABF results in rather wide null.

On the other hand, for broad array, similar to subarrayed broadband ABF, the subarrayed fast-time STAP should adopt time delays at subarray outputs to compensate phase difference. This is subarrayed fast-time STAP with broadband

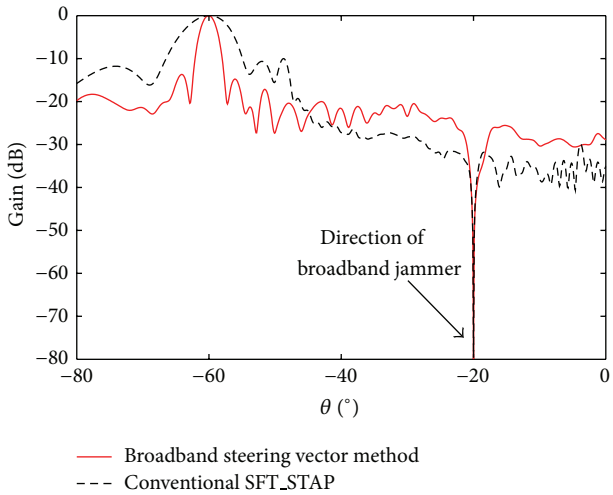

FIGURE 5: Adaptive pattern by broadband steering vector-based subarrayed fast-time STAP.

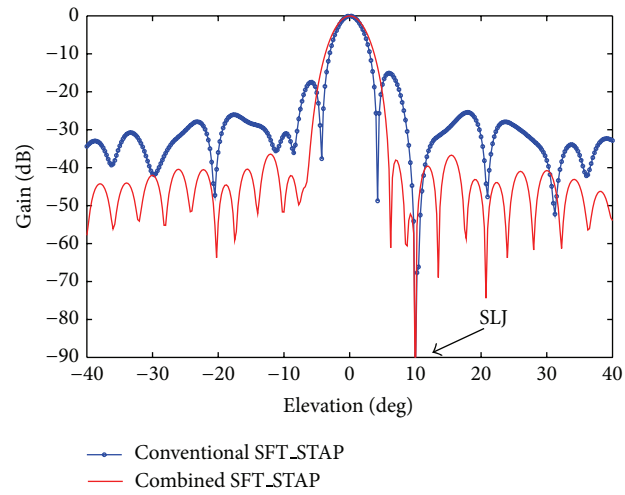

FIGURE 6: Comparison of combined subarrayed fast-time STAP with the optimum one.

steering vector method [50]. Here, broadband steering vector method modifies constraint condition of conventional LCMV criterion, so that the gain of the pattern in desired signal direction is a constant within the whole receiving bandwidth.

We give the simulation results, in which the parameters of array are set the same as Figure 3. The central frequency of the bandwidth of array is the same as that of the bandwidth of jammer. Adaptive pattern obtained with broadband steering vector method-based subarrayed fast-time STAP is illustrated in Figure 5 [50]. It is seen that the look direction and mainlobe shape are preserved, which is impossible for the conventional subarrayed fast-time STAP (conventional SFT_STAP for short).

The optimum adaptive weights of subarrayed fast-time STAP can be determined by the LCMV criterion [51]. However the PSL is very high which is similar to optimum subarrayed ABF. Therefore, we adopt the approach combining the optimum subarrayed fast-time STAP and subarrayed fast-time STAP with the quiescent pattern control capability, in order to make a trade-off between the PSL and the broadband jammer suppression capability.

The adaptive pattern in the case of broadband SLJ is given in Figure 6 [50]; meanwhile K_{Opt} is chosen to be 0.6 for the combined subarrayed fast-time STAP. It is seen that the PSL of combined subarrayed fast-time STAP is improved remarkably, namely, by 13.2 dB in comparison with the optimum one.

4. The Subarray Weighting-Based Sidelobe Reduction of Sum and Difference Beam

The sidelobe reduction of patterns is the basic task for the PAR systems. In this section, we deal with subarray weighting-based algorithms for the PSL reduction of sum and difference beam. The goal is to obtain a trade-off between hardware complexity and achievable sidelobe level.

One function of subarray weighting is to reduce the PSL of both the sum and the difference beam simultaneously for a monopulse PAR, in which digital subarray weighting substitutes the analog element amplitude weighting. Accordingly, hardware cost and complexity are greatly reduced.

In this section, two techniques are presented as follows.

4.1. Full Digital Weighting Scheme. This approach completely substitutes the element weighting adopting subarray weighting (for instance, a Taylor and Bayliss weighting for sum and difference beam, resp.). We assume that no amplitude weighting at element level is possible. The two schemes for determining subarray weights are as follows.

4.1.1. The Analytical Approach. The analytical approach includes two ways, namely, weight approximation and pattern approximation. The former makes the subarray weight to approximate the Taylor or Bayliss weight in LMS (least mean square) sense, while the latter makes the patterns obtained with the subarray weights approximate to that obtained by the Taylor or Bayliss weight in LMS sense [2].

The weight approximation-based subarray weights are determined by

Sum beam:

$$\mathbf{w}_{\Sigma\_\text{WA}}^{(\text{opt})} = \arg\min_{\mathbf{w}_{\Sigma\_\text{WA}}} \left\| \mathbf{T}\mathbf{w}_{\Sigma\_\text{WA}} - \mathbf{w}_{\text{Tay}} \right\|_2^2, \tag{7}$$

Difference beam:

$$\mathbf{w}_{\Delta\_\text{WA}}^{(\text{opt})} = \arg\min_{\mathbf{w}_{\Delta\_\text{WA}}} \left\| \mathbf{T}\mathbf{w}_{\Delta\_\text{WA}} - \mathbf{w}_{\text{Bay}} \right\|_2^2,$$
$$\mathbf{a}^H(\theta_0, \varphi_0)\left(\mathbf{T}\mathbf{w}_{\Delta\_\text{WA}}^{(\text{opt})}\right) = \mathbf{0}, \tag{8}$$

where $\mathbf{w}_{\text{Tay}}$, $\mathbf{w}_{\text{Bay}}$ denote Taylor weigh vector, Bayliss weigh vector, respectively.

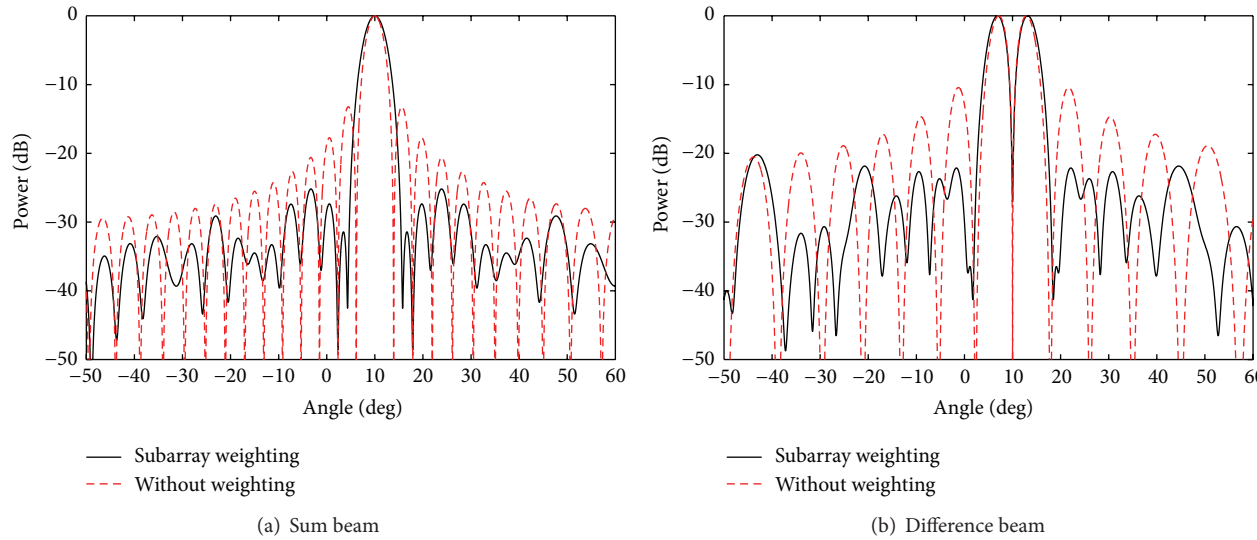

(a) Sum beam (b) Difference beam

Figure 7: Subarrayed weighting-based quiescent patterns.

Take the sum beam for example, the pattern approximation-based subarray weights are determined by

$$\mathbf{w}_{\sum\_\mathrm{PA}}^{(\mathrm{opt})} = \arg\min_{\mathbf{w}_{\sum\_\mathrm{PA}}} \int_{-\pi/2}^{\pi/2}\int_{-\pi/2}^{\pi/2} \left|\mathbf{w}_{\sum\_\mathrm{PA}}^{H}\mathbf{T}^{H}\mathbf{a}(\theta,\varphi) - \mathbf{w}_{\mathrm{Tay}}^{H}\mathbf{a}(\theta,\varphi)\right|^{2} \times P(\theta,\varphi)\,\mathrm{d}\theta\,\mathrm{d}\varphi, \tag{9}$$

where $P(\theta,\varphi)$ is the directional weighted function. It could adjust the approximation of pattern obtained by the pattern approximation method and the pattern obtained by the Taylor weights in a certain direction area which leads to better sidelobe reduction capability.

Assume a ULA with 30 omnidirectional elements with $\lambda/2$ of element spacing. The look direction is 10°, and the array is divided into 11 nonuniform subarrays. Figure 7 shows patterns obtained by pattern approximation method which are used for approximating the patterns obtained by −30 dB Taylor and −30 dB Bayliss weighting, respectively. The PSL is −25.18 dB for the sum beam (Figure 7(a)) which is improved by 11.95 dB compared with that without weighting, while PSL is −20.22 dB for the difference beam (Figure 7(b)) which is improved by 9.78 dB compared with that without weighting. It is seen that the PSL reduction effect of difference beam is inferior to the one of the sum beam for the subarray weighting method, since the constraint for the null restricts a further improvement of PSL.

Note the subarray weighting-based PSL reduction capability cannot be the same as that with element weighting, which is a price required for reducing the hardware cost. This approach is more suitable for the difference beam which is used for target tracking.

4.1.2. GA (Genetic Algorithm) . This approach optimizes the subarray weights using GA. The GA could achieve global optimum solution which is unconstrained by issues related solution.

Here, fitness function has a great influence to PSL reduction capability. We choose two kinds of fitness functions: (1) the weight approximation-based fitness function, that is, $f_{\mathrm{WA}} = \|\mathbf{T}\mathbf{w}_{\mathrm{sub}} - \mathbf{w}_{\mathrm{ele}}\|_2^2$, where $\mathbf{w}_{\mathrm{sub}}$ and $\mathbf{w}_{\mathrm{ele}}$ are the subarray weights and element weights, respectively; (2) the PA-based fitness function, namely, making PSL of pattern obtained by subarray weighting as low as possible, which turns to be more reasonable. Meanwhile, main beam broadening should be limited in a certain range. Furthermore, it should form a notch with enough null depth in a certain direction for the difference beam. For example, for difference beam, the fitness function is designed as $f_{\mathrm{patt}} = k_{\mathrm{SLL}}(\Delta_{\mathrm{SLL}})^2 + k_{\mathrm{BW}}(\Delta_{\mathrm{BW}})^2 + k_{\mathrm{ND}}(\Delta_{\mathrm{ND}})^2$, where Δ_{PSL}, Δ_{BW}, and Δ_{ND} are difference between expected value and practice value of PSL, beamwidth, and null depth, respectively, k_{SLL}, k_{BW}, and k_{ND} are used for adjusting the weighing coefficients of Δ_{SLL}, Δ_{BW}, and Δ_{ND}, respectively.

Adopting f_{weight} as fitness function brings high operating efficiency; however, the PSL reduction performance is unsatisfactory because only the weight vector is optimized. While adopting f_{patt} as the fitness function can improve the performance, because the PSL itself is optimized in this case. However, its drawbacks are that the genetic operation is easily constrained on local optimal solution and the computing efficiency is poor.

In order to overcome the limitation of two approaches mentioned above, we present an improved GA, that is, partition genetic process into two stages whose process is as below. The first stage is used for the preliminary optimization using f_{weight} as fitness function. Then we turn into stage 2 which is used for improving PSL reduction capability further; namely, according to descending order of fitness values of the first stage, select a certain scale of excellent filial generations among optimizing results to compose new

Table 2: The PLSs of sum beam with several approaches.

	Without weighing	Conventional GA (with fitness function f_{WA})	Conventional GA (with fitness function f_{patt})	Improved GA
PSL (dB)	−13.43	−26.18	−27.70	−27.77

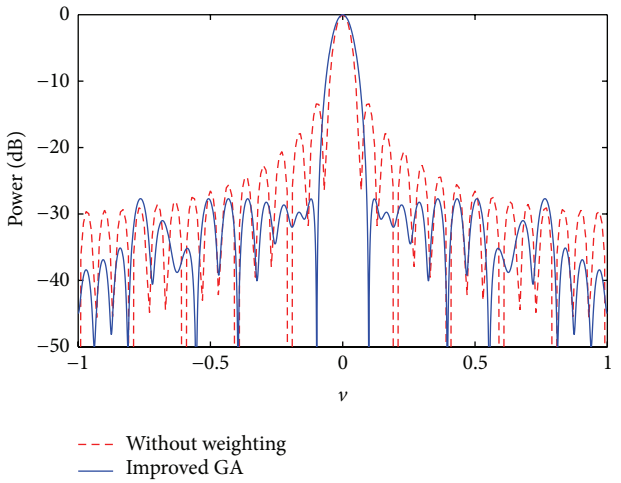

Figure 8: Sum patterns: improved GA.

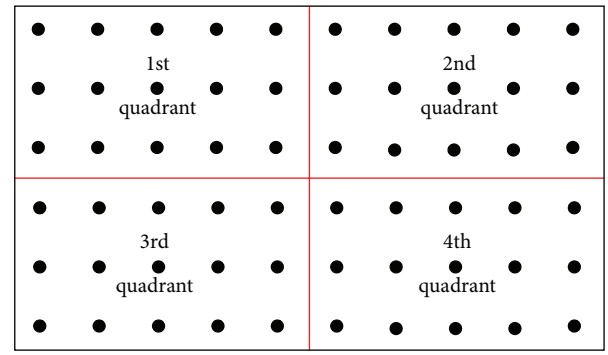

Figure 9: The division of planar array into four quadrants.

population. Afterwards, continue to optimize by using f_{patt} as fitness function.

There is a UPA containing 30 × 30 omnidirectional elements with the element spacing $d = \lambda/2$ in the direction of x and y. The beam direction is $(0^\circ, 0^\circ)$. The array is divided into 10 × 10 nonuniform subarrays. The improved GA-based subarray weights are used to approximate −30 dB Taylor weights, in which number of generations is 1300 in first stage and 20 in second one, respectively. Figure 8 reports the sum pattern; it is seen that obtained PSL is close to the expected −30 dB.

Table 2 shows the PSLs with several methods, in which PSL reduction capability with f_{patt} fitness function is better than that with f_{WA} (it is improved by 1.58 dB) for conventional GA. And PSL reduction performance of improved GA quite is close to the one of conventional GA with f_{patt} (meanwhile, improved GA enhances calculation efficiency greatly), which is degraded only by 2.23 dB compared with expected Taylor weight.

4.2. Combining of Element and Subarray Weighting. The scheme generates sum and difference channels simultaneously only using an analog weighting. In order to determine the analog weights, it is assumed that the supposed interferences locate within the sidelobe area of sum and difference beams [25]. Then the supposed interferences are adaptively suppressed (e.g., based on LCMV criterion). And the obtained adaptive weight is regarded as the desired analog weight. Furthermore, the subarray weighting is adopted; that is, analog weight is combined with the digital weights in order to improve the PSL reduction capability. The subarray weighting has two forms which are used for sum and difference beam, respectively. Then the subarray weights could be determined by the weight approximation or the pattern approximation approach, as mentioned in Section 4.1.

The literature [25] presented above-mentioned approach for the ULA. Next we focus on planar array [52]. Consider a UPA with $N_x \times N_y = N$ elements. First the array is divided into four equal quadrants as shown in Figure 9. And then we number the elements as $1 \le n \le N/4$ in the first quadrant, $N/4 + 1 \le n \le N/2$ for the elements in the second quadrant, $N/2 + 1 \le n \le 3N/4$ for the elements in the third quadrant, and $3N/4+1 \le n \le N$ for the elements in the fourth quadrant. The sum and difference channels are shown in Figure 10.

Assume coordinate of nth ($n = 1, \ldots, N$) element is (x_n, y_n). The analog weight is $\mathbf{w}_{ele} = \mu \mathbf{R}^{-1} \mathbf{a}(\theta_0, \varphi_0)$, where μ is a nonzero constant; $\mathbf{a}(\theta_0, \varphi_0)$ is the steering vector into the look direction; $\mathbf{R} = \mathbf{R}_{\mathbf{x}_\Sigma} + \mathbf{J}_\Delta \mathbf{R}_{\mathbf{x}_\Delta} \mathbf{J}_\Delta$ with $\mathbf{J}_\Delta = \mathrm{diag}(\underbrace{\mathbf{q}\ \mathbf{p}\ \cdots\ \mathbf{q}\ \mathbf{p}}_{N_y/2}\ \underbrace{\mathbf{p}\ \mathbf{q}\ \cdots\ \mathbf{p}\ \mathbf{q}}_{N_y/2})$, and $\mathbf{q}$ is $N_x/2$-dimensional unit row vector, while $\mathbf{p}$ is $N_y/2$-dimensional row vector in which every element is −1. Assuming the interferences are with uniform distribution, let $\mathbf{R}_{\mathbf{x}_\Sigma} = (r_{ik\_\Sigma})_{i,k=1,2,\ldots,N}$; then we have

$$r_{ik\_\Sigma} = \begin{cases} \pi\left(1 - R_\Sigma{}^2\right)\sigma_{I\_\Sigma}^2 + \sigma_n^2, & i = k \\ 2\pi e^{j\pi[(x_i - x_k)u_0 + (y_i - y_k)v_0](l_0 - R_\Sigma l_\Sigma)\sigma_{I\_\Sigma}^2}, & i \ne k \end{cases} \quad (10)$$

with $l_0 = J_1(c_{ik})/c_{ik}$, $l_\Sigma = J_1(c_{ik}R_\Sigma)/c_{ik}$, where $J_1(\cdot)$ is first order Bessel function of the first kind and $c_{ik} = 2\pi\sqrt{(x_i - x_k)^2 + (y_i - y_k)^2}/\lambda$; R_Σ is mainlobe radius of sum beam; $\sigma_{I\_\Sigma}^2$ is power of interference imposing on sum beam; σ_n^2 is thermal noise power. Similarly, we can obtain r_{ik_Δ} with $\mathbf{R}_{\mathbf{x}_\Delta} = (r_{ik\_\Delta})_{i,k=1,2,\ldots,N}$.

It should be pointed out that the PSL reduction effect with only analog weighting approach is determined by the selected design parameters, such as JNR and spatial distribution of supposed interferences.

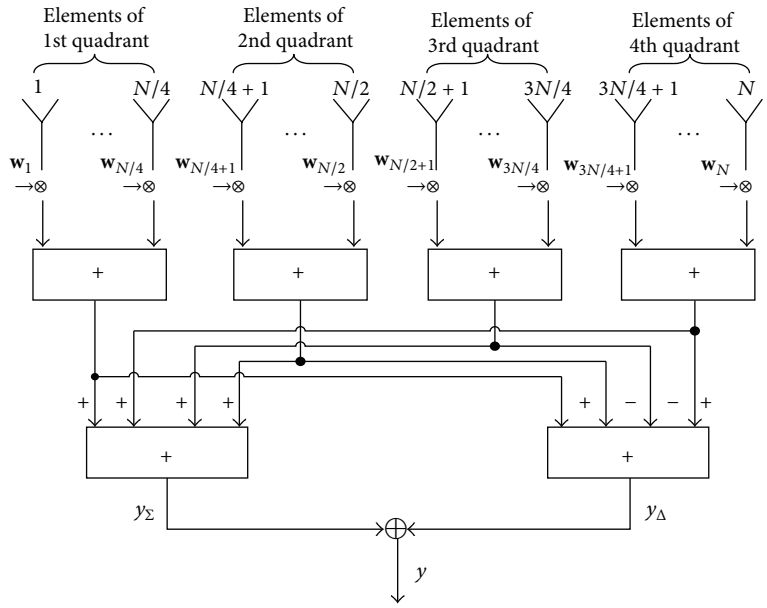

FIGURE 10: Construction of sum and difference channels.

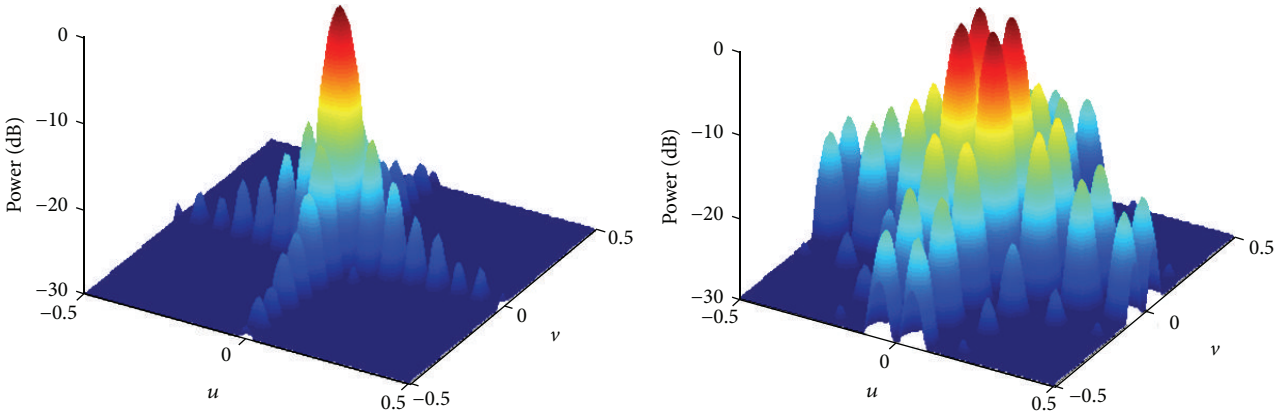

(a) Sum beam (b) Double difference beam

FIGURE 11: Patterns obtained by only analog weighting.

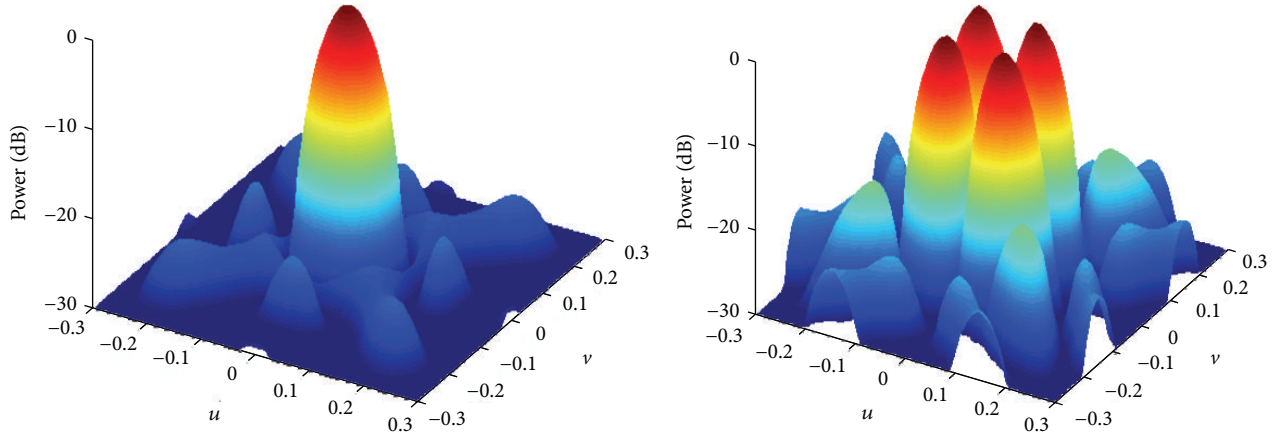

(a) Sum beam (b) Double difference beam

FIGURE 12: Patterns obtained by analog and digital weighting (with weight approximation approach).

Assume that a UPA consists of 30 × 30 elements on a rectangular grid at half wavelength spacing configured into 10 × 10 uniform subarrays. The look direction is (0°, 0°). For sum and double difference beam (double difference beam is useful for main beam ECCM application, for instance, the mainlobe canceller), the JNRs of supposed interferences are both of 30 dB. Figure 11 shows patterns generated by only analog weighting. The PSLs of the sum and difference pattern are −14.51 dB and −10.77 dB, respectively. Figure 12 shows the results of adopting both element weighting and weight approximation-based subarray weighting, in which the PSLs of sum and double difference patterns are improved by 8.34 dB and 5.27 dB, respectively, compared with Figure 11.

In fact the PSL reduction capabilities of weight approximation- and pattern approximation-based subarray weighting are quite close.

5. The Sidelobe Reduction for Subarrayed Beam Scanning

The look direction is usually controlled by phase shifters for PAR. However further subarrayed digital beam scanning may be required for forming multiple beams and many other applications which are used for a limited sector of look directions around the presteered direction.

Typically with subarrayed scanning, the PSL will increase rapidly with the scanning direction departing from the original look direction. The larger the scan angle is, the greater the PSL increase is [11]. Therefore the requirement for sidelobe reduction arises.

In this section, we discuss the PSL reduction approaches for subarrayed beam scanning, namely, beam clusters created at subarray level.

With subarrayed scanning, the resulting pattern is composed of the pattern of each subarray. Each subarray pattern has a high PSL which contributes to a high PSL of the array pattern. If pattern of each subarray would be superimposed properly in the main beam and has a low PSL, the PSL of the array pattern could be reduced effectively.

Therefore, one can post-process the subarray outputs using a weighting network, consequently creating new subarrays with the patterns with similar shape within the main beam and with PSLs as low as possible. The starting point is to make the new subarray patterns to approximate the desired one.

The natural form of desired subarray pattern is the ISP (ideal subarray pattern) which is constant within the mainlobe and zero else [11]. It has two kinds of forms: (1) projection of mainlobe in array plane is a rectangular area, and (2) projection of mainlobe is a circular area.

As an example, assume that a UPA consists of 32 × 34 omnidirectional elements on a rectangular grid at half wavelength spacing. A −40 dB Taylor weighting is applied in both x and y directions. The array is divided into 6 × 6 nonuniform subarrays and each of which is a rectangular array. Assume $(u_0, v_0) = (-0.5, 0)$.

By using the ISP based on rectangular projection, we give an example for reducing the sidelobes in Figure 13(a). Obviously, the shape and beamwidth of the main beam of all subarrays are very similar, but the gain of the different subarrays makes a great difference in the results. Figure 13(b) shows patterns obtained by ISP based circular projection. Obviously, the shape, the beamwidth, and the gains of the main beam of all subarrays are very similar, which is superior to rectangular projection method.

Figure 14 shows array patterns after scanning carried out in u direction. Subplots (a), (b), and (c) show the patterns obtained without the weighting network processing, with ISP based rectangular projection and ISP based on circular projection, respectively. The different curves are given for nonscanning and scan angles of 0.5 Bw and 1.0 Bw, respectively, where Bw is the 3 dB beam width. Compared to the case without-weighting network, for ISP based on rectangular projection the PSL is reduced by 1.34 dB for 0.5 Bw scanning and 1.72 dB for the 1 Bw, while for ISP based circular projection the PSL is reduced by 1.99 dB and 2.39 dB, respectively.

It is seen from above-mentioned examples that the PSL reduction capability with ISP is not satisfied. For the reason, we adopt GSP- (Gaussian subarray pattern-) based approach [53]. Therein desired pattern is the Gaussian pattern, which is more smooth than the ISP [11].

The result obtained with the GSP approach is shown in Figure 15. Comparing Figure 15 with Figure 14(b), we see that the PSL by GSP is improved obviously compared with ISP based rectangular projection; namely, PSL is reduced by 1.49 dB for the 0.5 Bw scanning and 2.05 dB for the 1 Bw, respectively. Consequently, the GSP improves remarkably ISP as PSL of the latter is only reduced by more than 1 dB compared with non-weighting network; meanwhile the computational burden is equivalent to the latter [53].

6. The Subarrayed Adaptive Monopulse

In order to ensure the accuracy of angle estimation of monopulse PAR in jammer environments, we should adopt subarrayed adaptive monopulse technique. The subarrayed ABF can improve SINR and detection capability. However, under circumstances of MLJ (mainlobe jamming) the adaptive null will distort the main beam of pattern greatly, thus leading to serious deviation of the angle estimation. Thereby, the subarrayed adaptive monopulse should be applied.

Existing approaches usually take the adaptive patterns into account to avoid the degradation of monopulse performance near the null. For example, one can use LMS-based target direction search to determine adaptively the weights of optimum difference beam [54]. This kind of methods needs to adopt the outputs of the sum and difference beam to achieve the corrected monopulse ratio and it needs higher computational cost. Subarrayed linearly constrained adaptive monopulse is generalized from the linearly constrained adaptive monopulse [55]. But it reduces degree of freedom by adopting adaptive difference beam constraints.

The reined subarrayed adaptive monopulse methods with higher monopulse property have been suggested, for example, the approximative maximum-likelihood angle estimators

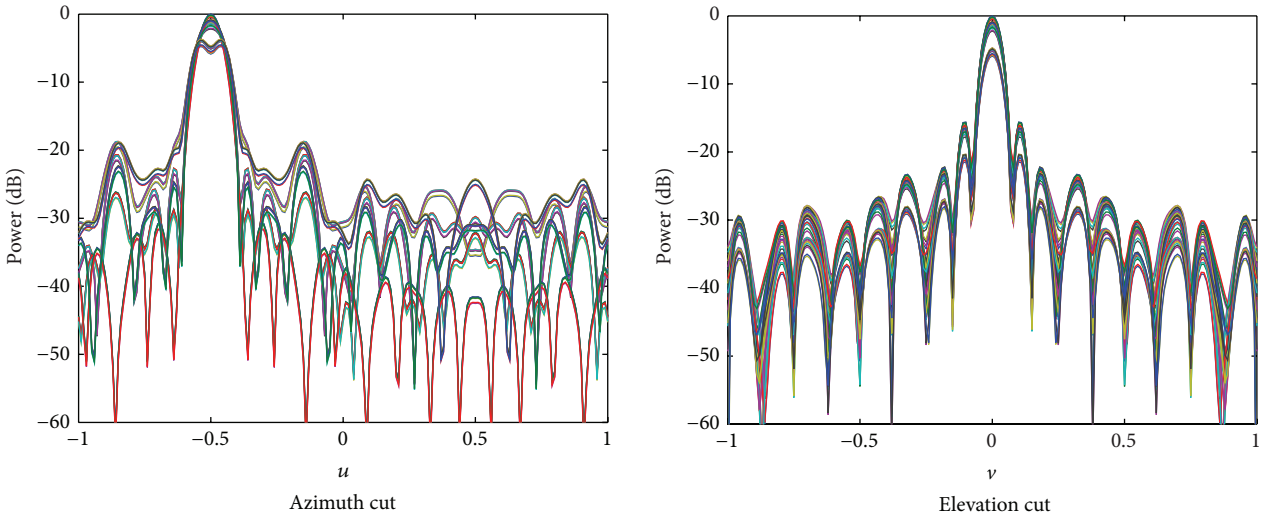

(a) Rectangular projection method

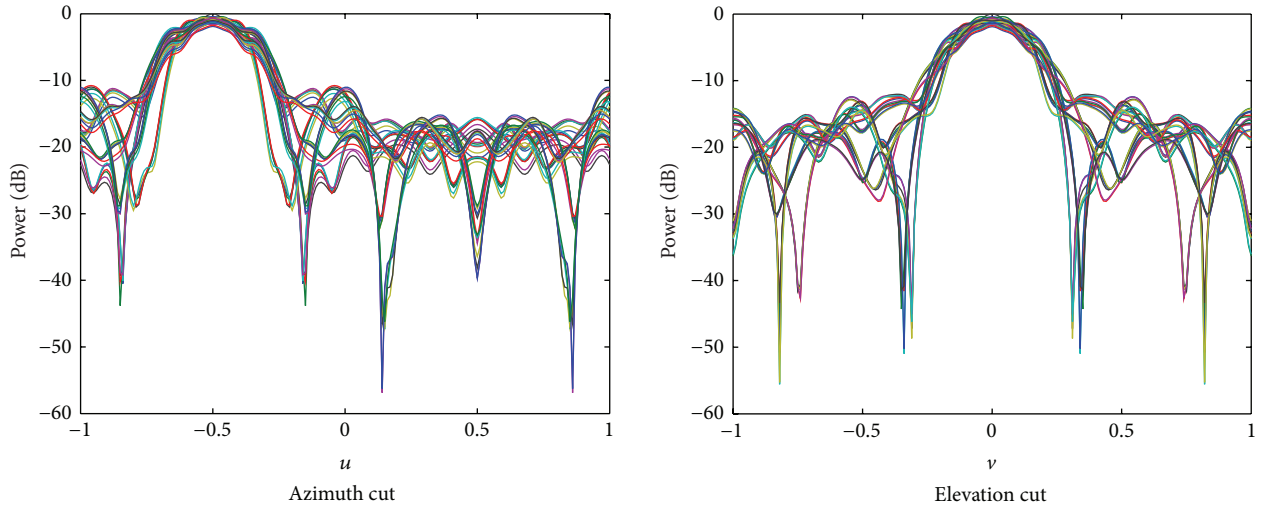

(b) Circular projection method

Figure 13: Subarray patterns obtained by ISP.

[12, 13, 15, 16] proposed by Nickel. In this section, we focus on two-stage subarrayed adaptive monopulse. Here we improve the conventional two-stage subarrayed adaptive monopulse which is an extension of the two-stage adaptive monopulse technique [56].

The realization process of the two-stage subarrayed adaptive monopulse is as follows: firstly, the subarrayed ABF is used to suppress the SLJ, while maintaining the mainlobe shape; secondly, the MLJ is suppressed, while maintaining the monopulse performance; that is, the jammers are canceled with nulls along one direction (elevation or azimuth) and undistorted monopulse ratio along the orthogonal direction (azimuth or elevation) is preserved. The two-stage subarrayed adaptive monopulse requires four channels, in which the delta-delta channel is used as an auxiliary channel for the mainlobe cancellation.

However, the method possesses two limitations: (1) after the first-stage processing, the PSLs of patterns increase greatly, and (2) the monopulse performance is undesirable, for there exists serious distortion in deviation of the look direction for adaptive monopulse ratio; the reason is that the MLM (mainlobe maintaining) effect is not ideal. Therefore, in the first-stage processing, subarrayed optimum ABF is substituted by MOD; consequently, the monopulse performance would be improved greatly [57].

Suppose a rectangular UPA with 56×42 elements and the element spacing is $\lambda/2$. A -40 dB Taylor weighting is applied in x and a -30 dB in the y direction. Array is partitioned into 6×6 nonuniform subarrays and each subarray is a rectangular array: $(\theta_0, \varphi_0) = (0^\circ, 0^\circ)$. Assuming that MLJ and SLJ are located at $(1^\circ, 2^\circ)$ and $(10^\circ, 15^\circ)$, respectively, then all the JNRS are 30 dB.

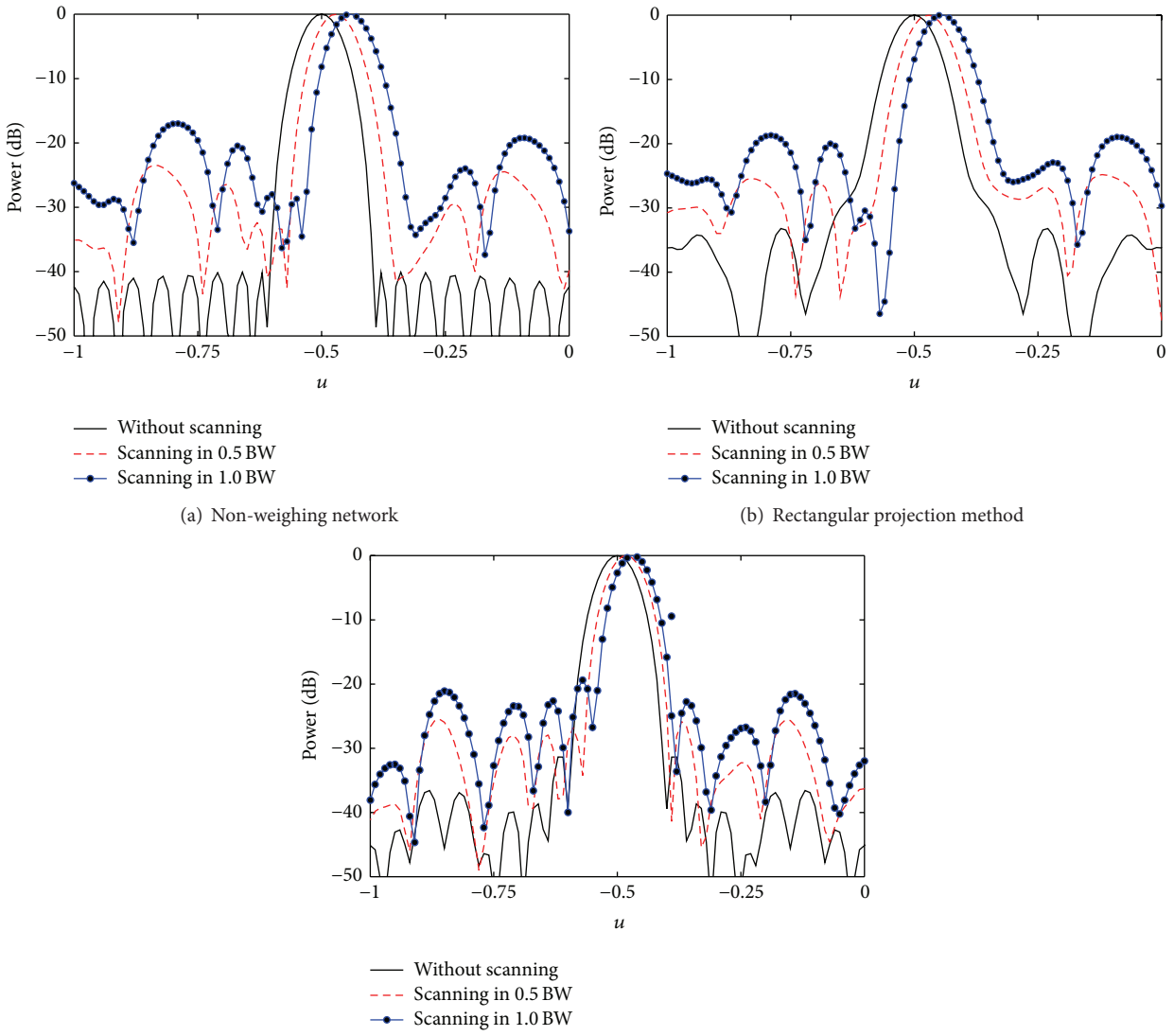

(a) Non-weighing network

(b) Rectangular projection method

(c) Circular projection method

FIGURE 14: Array patterns with beam scanning obtained by ISP method (azimuth cut).

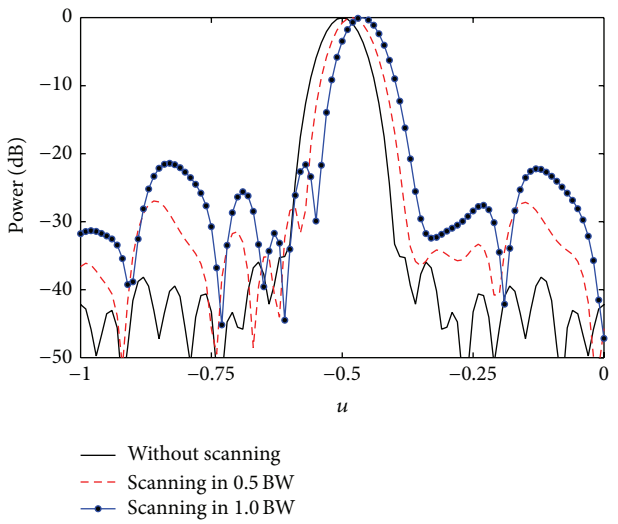

FIGURE 15: Array patterns with beam scanning obtained by GSP (azimuth cut).

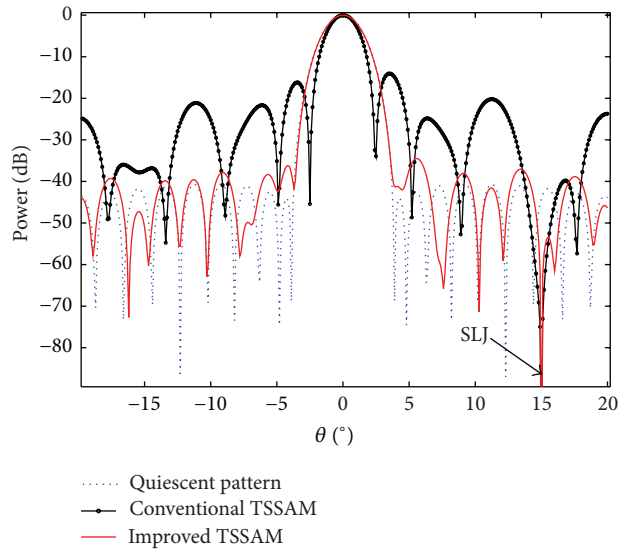

Figure 16: Adaptive patterns of elevation sum beam obtained by first-stage adaptive processing.

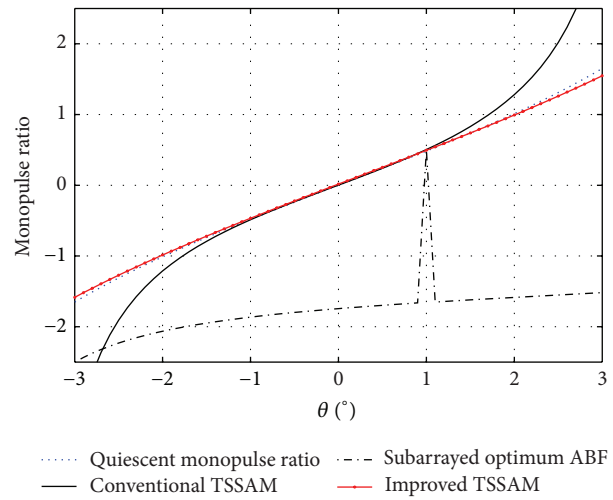

Figure 17: Elevation monopulse ratio obtained by two-stage adaptive processing.

Next we illustrate the simulation results taking the elevation direction as an example. Figure 16 is the cut of the adaptive patterns of elevation sum beam applying first-stage processing. It is obvious that the conventional two-stage subarrayed adaptive monopulse (TSSAM for short), namely the subarrayed optimum ABF combined with MLM obviously increases the PSL, compared with the quiescent pattern, and the mainlobe width shows apparent reduction, which leads to the distortion of adaptive monopulse ratio around the look direction. The PSL is improved greatly by using the MOD, and more important the remarkable improvement of the MLM effect makes the mainlobe shape close to that of the quiescent pattern; therefore a greater improvement of adaptive monopulse ratio can be obtained.

Figure 17 presents an elevation monopulse ratio obtained by the two-stage subarrayed adaptive monopulse. Let $u = \cos\theta \sin\varphi$ and $v = \sin\theta$, where φ and θ are the azimuth and elevation angle correspondingly. The monopulse ratio along elevation direction is $K_E(u,v) = F_{\Delta_E}(u,v)/F_{\sum}(u,v)$, where $F_{\sum}(u,v)$ and $F_{\Delta_E}(u,v)$ denote the pattern of sum beam and elevation difference beam, respectively. The two-dimensional antenna patterns are separable; therefore, $K_E(u,v) = F_{\sum_A}(u) F_{\Delta_E}(v)/[F_{\sum_A}(u)F_{\sum_E}(v)] = F_{\Delta_E}(v)/F_{\sum_E}(v)$ [56].

Since the subarrayed optimum ABF combined with MLM is used in the first-stage processing, the monopulse ratio deviated from the look direction shows serious distortion. Undoubtedly, the MOD combined with MLM is an appropriate choice to enhance adaptive monopulse ratio, for its similarity to quiescent monopulse ratio and the small distortion when deviated from the look direction. And the relative error of adaptive monopulse ratio with improved two-stage monopulse (MOD+MLM for first-stage processing) is only 3.49% compared with quiescent monopulse ratio when the elevation is -2.7°, while the conventional two-stage monopulse (subarrayed optimum ABF+MLM for the first-stage processing) is as much as 69.70%. So, improved method monopulse reduces error of monopulse ratio greatly compared with conventional method. The numerical results demonstrate that, in the range of 3 dB bandwidth of patterns, for the improved method monopulse, the relative error of adaptive monopulse ratio is less 1% and even reaches 0.01% compared with quiescent monopulse ratio.

Two-stage subarrayed adaptive monopulse integrates several techniques, including subarrayed ABF, MLM, quiescent pattern control, and four-channel MJC. The SLJ and MLJ are suppressed, respectively, so it is unnecessary to design the sophisticated monopulse techniques to match the mainlobe of patterns.

For the wideband MLJs, the SLC type STAP can be used to form both sum and difference beam. If auxiliary array is separated from the main array by distances that are sufficiently large, the array can place narrow nulls on the MLJ while maintaining peak gain on a closely spaced target [58]. Consequently, it can suppress MLJs effectively while preserving superior monopulse capability.

7. The Subarrayed Superresolution

To address angle superresolution issues, a variety of methods have been developed. This paper only focuses on subarrayed superresolution. In this section, two types of the approaches are described: the first refers to the narrowband superresolution; the second approach presents the broadband superresolution [6].

7.1. The Subarrayed Superresolution. The subarrayed superresolution direction finding could be achieved by extending the conventional superresolution algorithms into the subarray level. However, this kind of algorithms has to calibrate the whole array manifold. But for the active calibration technique the realization is very complicated and costly, while for the self-calibrate solutions there are limitations, for example, difficulty of implementation; high computational burden (some algorithms are many times more than original

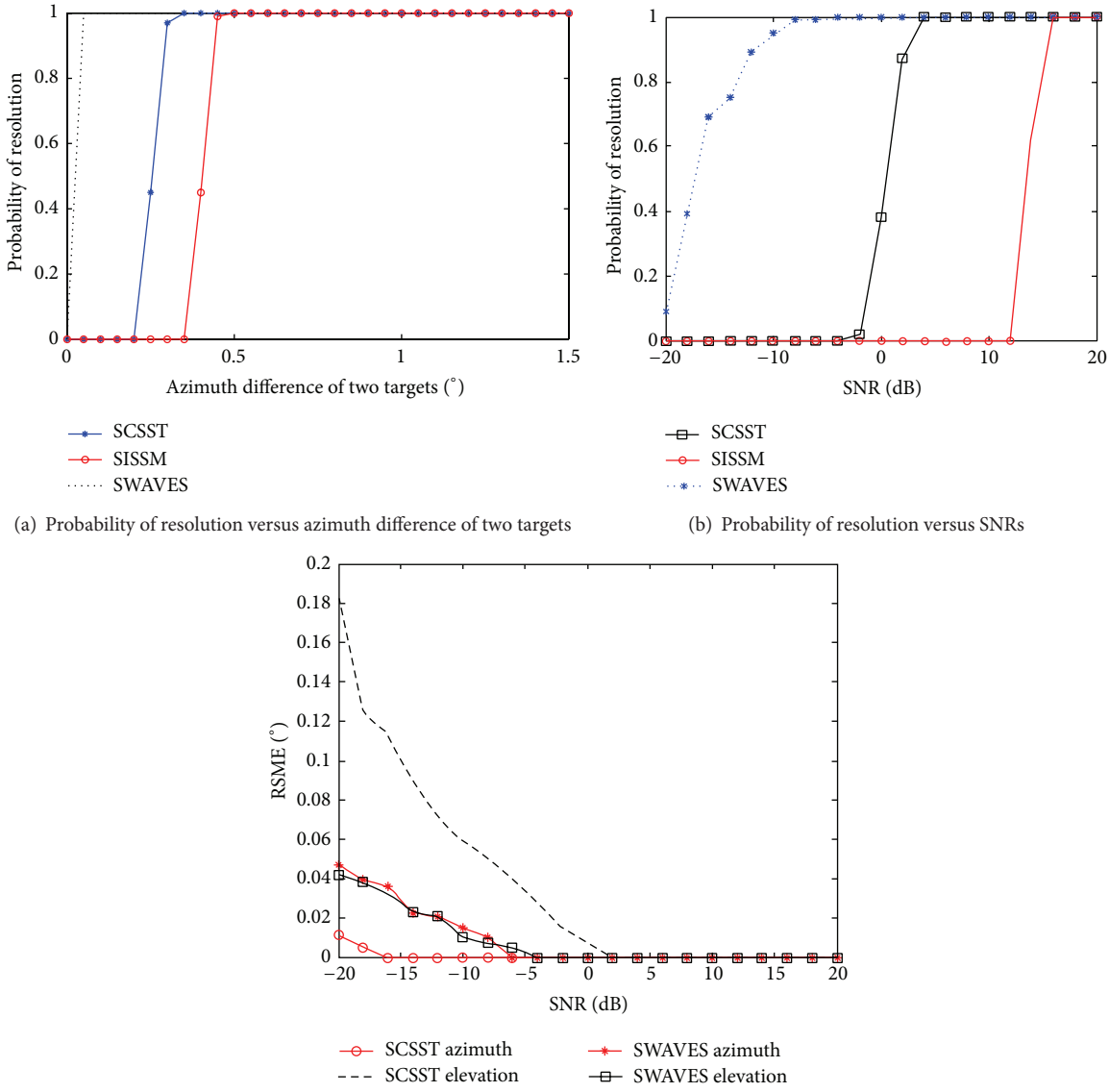

(a) Probability of resolution versus azimuth difference of two targets

(b) Probability of resolution versus SNRs

(c) The s.t.d of direction finding

Figure 18: Contrast of performances of three broadband subarrayed superresolution algorithms.

superresolution algorithms even); the convergence problems for some iterative algorithms; the performances are limited in the case of a lot of array position errors; some are only effective for specific errors of one or two kinds only [59].

Thus, simplified array manifolds can be used. The essence of these methods is to treat the whole array as a super-array and each subarray as a superelement. The idea is to approximate the patterns at subarray outputs by those of superelements located at the subarray centres [19]. The simplified array manifolds are only determined by phase centers and gain of subarrays [19]. Because the calibration needs to be implemented only inside the subarrays, the calibration cost and complexity are reduced greatly.

These methods can eliminate uncertain information in sidelobe area. The available region of direction finding of them is within 3 dB beamwidth of patterns around the center of the look direction. However, combined with beam scanning by element phase shifting, superresolution can be achieved in any possible direction, that is, make the superresolution be carried out repeatedly by changing look direction. The advantage is suppressing sidelobe sources in complicated situation such as multipathway reflection; consequently, number of sources and dimension of parameter estimation are reduced and the process of superresolution is simplified [19]. Meanwhile we can use beam scanning to find the area with no signal source and wipe it off in advance; therefore 2-D peak searching cost is reduced greatly.

The available direction finding area of direct simplified array manifold-based subarrayed superresolution is fixed which cannot be adjusted and the sidelobe sources cannot be suppressed completely. Changing subarray patterns can overcome the limitations, but it is unable to be achieved by

restructuring the subarray structure. The subarray structure is an optimized result based on various factors and hardware is fixed. Therefore, we post-process the subarray outputs by introducing a weighting network which constructs required new subarray patterns. This kind of methods improved the flexibility of array processing greatly and the optimization of subarrays for different purpose and distinct processing tasks can be achieved based the same hardware [19].

Compared with the method based direct simplified array manifold, the ISP and GSP methods can adjust the available region of direction estimation and suppress sidelobe sources better [19, 60, 61]. On the other hand, compared with the ISP and GSP methods, the approximate ISP and approximate GSP methods reduce the computational cost greatly, while the precision of direction finding and resolution probability are very close to ISP and GSP [62, 63], respectively.

7.2. The Broadband Subarrayed Superresolution. The subarrayed superresolution approaches presented in the Section 7.1 are based on the scenario of narrowband signals. Next let us consider the broadband subarrayed superresolution which includes three kinds of approaches, namely, subband processing, space-time processing, and subarray time-delaying processing [6].

The subarrayed ISSM (incoherent signal subspace method), subarrayed CSST (coherent signal subspace transform), and subarrayed WAVES (weighted average of signal subspace) translate broadband problems into a subband processing. All these algorithms need to make delay-weighing for outputs of subbands. The subarrayed ISSM only averages the direction finding results of each subband obtained by subarrayed MUSIC. The subarrayed CSST and subarrayed WAVES should choose the suitable focusing transformation matrix and therefore need to preestimate source direction. If the preestimated direction is erroneous, the direction finding performance will be degraded. The subarrayed WAVES determines a joint space from all subspaces of subband covariance matrix, which is only one representative optimum signal subspace [6]. The mentioned-above subband processing methods can be combined with simplified array manifolds. Consequently, the broadband subarrayed superresolution can be achieved.

The broadband superresolution based on subarray time delay does not need any subband processing. Accordingly, it has less calculation which is easy to be implemented but needs a focusing transform. For the simplified array manifold-based approaches, they have better performance if the preestimated target direction is near the look direction; otherwise the performance would be degraded rapidly.

The narrowband subarrayed superresolution can be extended to the space-time superresolution (such as the subarrayed space-time MUSIC). Through compensating the phase using a subarray delay network, this kind of algorithms reduces the frequency-angle ambiguities. Then use the space-time steering vector to calculate the space-time covariance matrix and extract the dominant signal subspace [6]. The space-time broadband subarrayed superresolution does not need any focusing transform and direction preestimation, but the computation is costly.

To give an example, suppose a UPA with $19 \times 43 = 817$ elements, and the element spacing is $\lambda_0/2$. A -40 dB Taylor weighting is applied in x and a -30 dB in the y direction. Array is partitioned into $7 \times 11 = 77$ nonuniform subarrays and each subarray is a rectangular array. Assume look direction is $(5^\circ, 45^\circ)$. The sources are incoherent, broadband with $B = 0.2 f_0$ and with equal power. Suppose there are two targets; in both the elevation is 43.0° and the azimuth difference varies from 5.0° to 0° and SNR (signal-to-noise ratio) is 0 dB.

Two targets are deemed to be separable if their peak values of spatial spectrum both are greater than the value in the central direction of targets. Namely, targets are resolvable if the following two conditions are both met: $P(\theta_1) > P((\theta_1 + \theta_2)/2)$ and $P(\theta_2) > P((\theta_1 + \theta_2)/2)$, where θ_1 and θ_2 are directions of spectrum peaks of the targets, respectively. And the probability of resolution is the probability that the two targets are successfully resolved.

Figure 18(a) plots the probability of resolution curves obtained by several algorithms [64]. It can be seen that the angle resolution capability of subarrayed WAVES (SWAVES for short) is the best, while subarrayed ISSM (SISSM for short) is the worst. Assuming two targets located at $(4.0^\circ, 45.0^\circ)$ and $(5^\circ, 43.0^\circ)$, Figure 18(b) shows the curves of the probability of resolution versus SNRs. From the figure it can be found that probability of resolution of subarrayed WAVES is the best, followed by subarrayed CSST (SCSST for short), and subarrayed ISSM is the worst. Figure 18(c) gives the curves of RMSE of direction estimation versus SNRs, in which RMSEs are the average value of the estimations of the two targets [64].

8. Subarray Configuration Optimization for ECCM

For the PAR equipped with ABF, the optimization of subarray configuration is a key problem and challenge in the field of the SASP.

For its obvious influence on the performance of PAR, the optimization of subarray configuration can bring much improvement of the system performances such as sidelobe level, detection capability, accuracy of angle estimation, ECCM capability (anti-MLJ), and so forth. The subarray division is a system design problem; the optimized result has to take into account various factors. However, different capabilities may be contradictory mutually.

There are different solutions to this contradiction. In this section we briefly overview the MOEA (multiobjective evolutionary algorithm) procedure working on this issue. MOEA might make an optimal trade-off between above-mentioned capabilities.

The objective functions in the MOEA could be the mean P_d for different positions of the target, the mean CRB (Cramer-Rao Bound) of the target azimuth/elevation estimation, the mean PSLs of sum adapted pattern in the azimuth/elevation plane, and so forth [28]. But the set of optimum solutions is obtained after the subarray optimization through MOEA. Therefore, we need to determine posteriorly an optimized array through optimizing the

specific capability or introducing constraints (such as the geometric structures or the realization cost and complexity of array).

On the other hand, several issues should be considered on engineering realization: for example, all the subarrays are nonoverlapped and array is the fully filled, subarray configuration is relatively regular, and all elements inside a subarray are relatively concentrative (subarray's shapes should not be disjointed). Therefore, multiple constraints should be set during the process of genetic optimization.

The process of optimizing subarray is quite complicated for the great amount of elements in a PAR and the large searching space. Thus we can adopt the improved GA to make optimizing with a characteristic of adaptive crossover combination, which is based on the adaptive crossover operator; this will result in remarkable enhancement on convergence speed of optimization and calculation efficiency [65].

Suppose a UPA with $30 \times 32 = 960$ omnidirectional elements and element spacing is $\lambda/2$. A -40 dB Taylor weighting is applied in x and in the y direction. The subarray number is 64, $(\theta_0, \varphi_0) = (0^\circ, 0^\circ)$. The original subarray structure is selected randomly. Suppose that the direction of the MLJ is $(1^\circ, 1^\circ)$ and JNR = 35 dB.

We optimize the five objective functions simultaneously based on the MOEA. Hereinto, the first objective function is the PSL of adapted sum pattern in $u = 0$ cut. Figure 19(a) shows the adapted sum pattern obtained by the optimized subarray configuration and the original one, respectively. Here the original and optimized PSL are -12.36 and -22.37 dB, respectively; namely, the PSL is improved by 10.01 dB. The second objective function is the PSL of adapted sum pattern in $v = 0$ cut. Figure 19(b) shows the adapted sum pattern cut obtained by the optimized subarray configuration and the original one, respectively, in which the original and optimized PSL are -8.93 dB and -15.98 dB, respectively; therefore the PSL is improved by 7.05 dB. Note here the PSL is the third high sidelobe in the patterns, because the second one is caused by adaptive null.

On the other hand, for the PAR with subarrayed ABF, the ideal optimum subarray configuration should keep system's performances be optimal for various interference environments interference environments. But this is impossible to realize in principle.

9. The Subarrayed Processing for MIMO-PAR

Historically, the SASP techniques are mainly used for the PAR systems. In this section, we discuss the concept of the SASP suitable for MIMO-PAR system. Creating this technique is an impetus following from previous sections.

The MIMO structure is impracticable when the array is composed of hundreds or thousands of elements due to the huge quantity of independent transmitting signals and transmitting and receiving channels. Hardware cost and algorithmic complexity will exceed the acceptable level.

Therefore, we present the subarrayed MIMO-PAR. It is an extension of the subarrayed PAR. The MIMO-PAR is the combination of MIMO radar and PAR: the array is divided into several subarrays; inside each subarray a coherent signal is transmitted, working as PAR mode; orthogonal signals are transmitted between subarrays to form a MIMO system. The MIMO-PAR presented in this paper adopts Tx/Rx array modules, and transmitting and receiving arrays have the same subarray configuration, while both at the transmitting and receiving ends the SASP techniques are be applied.

9.1. The Characteristics of MIMO-PAR. The features of MIMO-PAR are listed as follows.

(1) It maintains advantages of MIMO radar as well as the characteristics of PAR (such as the coherent processing gain).

(2) Compared with MIMO radar, the MIMO-PAR reduces the cost and complexity of the hardware (the number of the transmitting and receiving channels) and the computational burden greatly. For example, the dimension of optimization algorithms for designing transmitting signals is reduced to subarray number, while it is the same as the element number in MIMO. Typically element number has an order of magnitude from several hundreds to several thousands and subarray number is only a few dozens of magnitude.

(3) Hardware cost and algorithm complexity can be flexibly controlled by adjusting the number of the subarrays. The ability of coherent processing (SNR) and the characteristics of waveform diversity (angle resolution) can be compromised by adjusting the subarray structure and subarray number.

(4) Compared with MIMO radar, the transmitting signals of different subarrays can be combined with independent beam look directions to improve the capability of beam control, producing more flexible transmitting beam patterns, thus improving the flexibility of object tracking.

(5) The characteristics with further advantages over MIMO radar, such as lower PSL of total pattern, can be achieved by design of the weighting of subarrayed transmitting/receiving BF. Moreover, MIMO-PAR can enhance the anti-jamming capability and generate higher output SINR under strong interference, and realize low PSL without expense of mainlobe gain loss.

(6) The performance of the system can be enhanced by optimizing the structure of subarray, such as transmitting diversity, SNR, PSL of total pattern, the performance of transmitting beam, and the ECCM capability.

(7) The exiting research achievements related to receiving SASP for PAR can be generalized to the MIMO-PAR. This is a promising direction of further studies.

(8) The configuration of MIMO-PAR with Tx/Rx modules can be easily made compatible with existing subarrayed PAR.

9.2. The Research Topics of SASP for MIMO-PAR. The research topics are as follows.

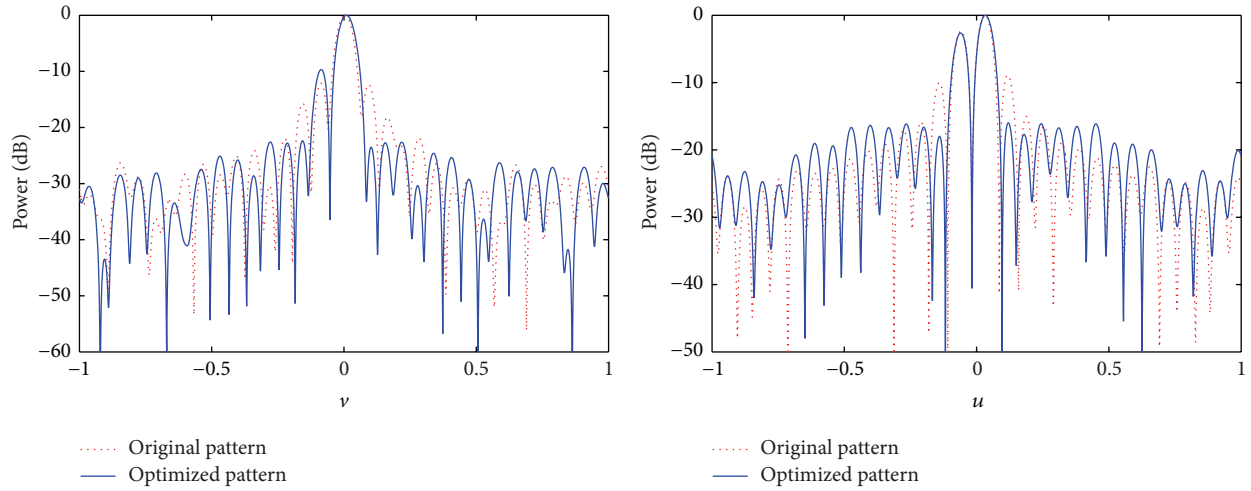

(a) First objective function: sum adapted pattern in $v = 0$ cut

(b) Second objective function: sum adapted pattern in $u = 0$ cut

Figure 19: Optimized results based on MOEA.

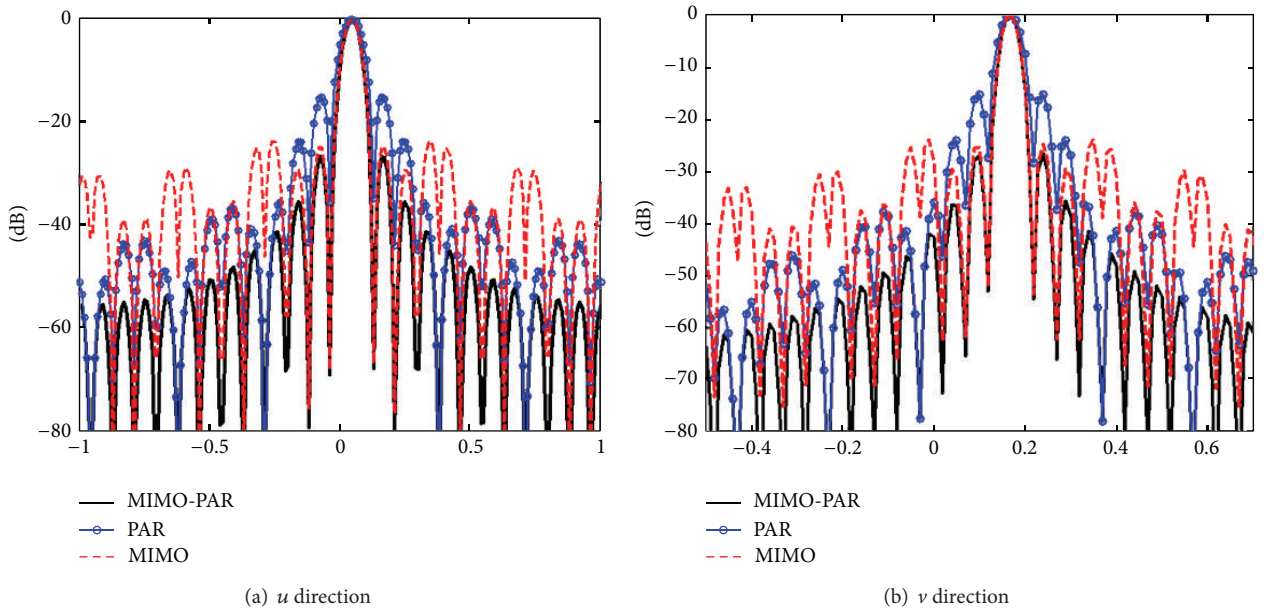

(a) u direction

(b) v direction

Figure 20: Total patterns of PAR, MIMO, and MIMO-PAR.

9.2.1. Subarrayed Transmitting/Receiving BF

(1) Subarrayed Transmitting BF. The use of robust subarrayed transmitting BF can minimize the transmitted power. The starting point is minimizing the norm of the transmitting BF weight vector while restricting the upper bound of sidelobes [66].

(2) Subarrayed Receiving BF. The subarrayed ABF for PAR is described in Section 2 can be employed for MIMO-PAR. Furthermore, the subarrayed LSMI and subarrayed CAPS (constrained adaptive pattern synthesis) and so forth [1] can also be applied to MIMO-PAR.

(3) The Characteristic of the Transmitting/Waveform Diversity/Receiving Total Pattern. The virtual array steering vector of the MIMO-PAR is decided by the coherent processing gain vector, the waveform diversity vector, and the steering vector of the receiving array. And the total patterns are the production of transmitting pattern, wave diversity patterns, and receiving patterns.

Assume a UPA of Tx/Rx community with 960 omnidirectional elements on a rectangular grid at half wavelength spacing. The array is divided into $8 \times 8 = 64$ uniform subarrays, each of which is a rectangular array. Figure 20 illustrates the total pattern for the three radar models [67]. Table 3 shows the results of the comparison. It is seen that

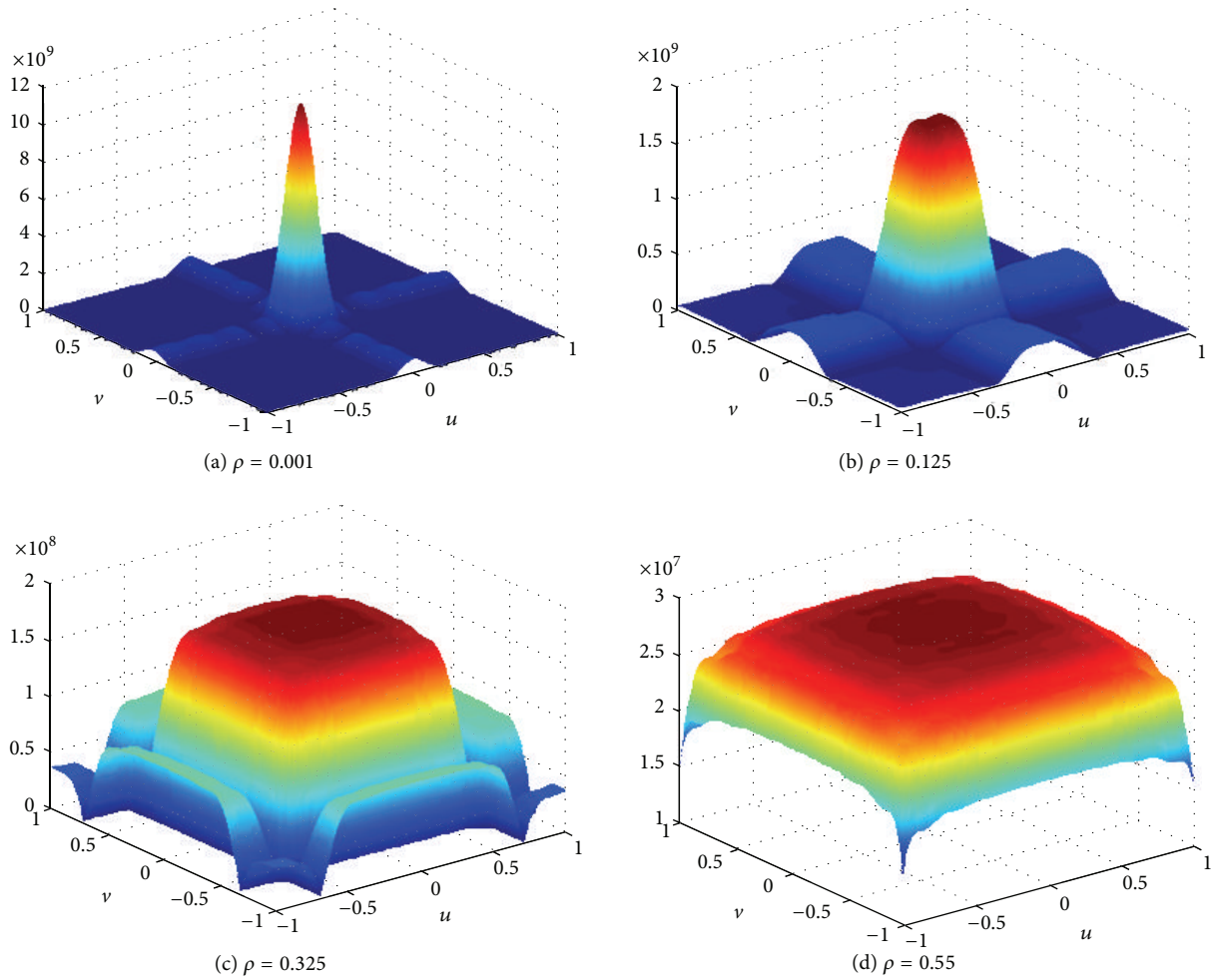

Figure 21: Transmit beam patterns based on synthesis of subarray transmitted signal.

Table 3: PSLs of total pattern for different radar models (dB).

Radar model	PAR	MIMO	MIMO-PAR
PSLs in u direction	−15.00	−24.66	−26.56
PSLs in v direction	−15.16	−25.26	−26.95

MIMO-PAR is superior to the PAR and the MIMO in terms of the PSL.

9.2.2. Synthesis of Transmitting Beam Pattern. The rectangle transmitting beam pattern can be used to radiate the maximum transmitting energy to interesting areas, so as to improve the exploring ability. As a result, a rectangle transmitting beam pattern can be synthesized from cross-correlation matrix of transmit signals [68].

The transmitting beam control includes two scenarios. (1) Each subarray has different beam directions to form a broad transmitting beam (for radar search mode). (2) Each subarray has the same beam direction to focus on transmitting beam (for tracking mode).

Aiming at a UPA, Figure 21 shows the transmitting beam patterns with different signal correlation coefficient ρ [69]. We observe that the beam width can be adjusted.

The performance evaluation of transmitted signal includes (1) orthogonality and (2) range resolution and multiple-target resolution (pulse compressing performance). On the other hand, the orthogonality degrades with increase of the subarray number.

9.2.3. Optimization of the Subarray Configuration. In the MIMO-PAR, when the element number and subarray number are fixed, the subarray structure has a significant impact on the system performance. Then the subarray structure has to be optimized. While in the MOEA method, the following constraints can be chosen as objective functions: (1) the waveform diversity capability, (2) the coherent processing gain, (3) the PSL of the total pattern in elevation direction, (4) the PSL of the total pattern in azimuth direction, and (5) the RMSE of the transmitting beam pattern and the rectangular pattern.

10. Conclusions and Remarks

In this paper, we describe some aspects of the SASP. From these investigations, we draw the concluding remarks as follows.

(1) For the SASP the achievable capabilities in application are constrained by some hardware factors, for example, channel errors.

(2) The amalgamation as well as integration of multiple SASP techniques is a trend, such as the combination of subarrayed ABF, adaptive monopulse, and superresolution. Consequently, the performance of the SASP could be improved.

(3) The subarray optimization is still a complicated and hard problem, compared with the algorithms.

(4) The extension of the SASP into MIMO-PAR could promote and deepen development of the SASP.

Furthermore, we point out the problems to be dealt with. The challenging works are in the following areas.

(1) The more thorough study of subarray optimization should be carried out. It is important for improving capabilities of system (including ECCM).

(2) The SASP for anti-MLJs is still a hard research topic.

(3) The SASP techniques for the thinned arrays should be further developed.

(4) At present, the research focuses mainly on the planar arrays which are only suitable for small angle of view (for instance, ±45°). The SASP should be extended to the conformal arrays (e.g., seekers).

List of Acronyms

ABF: Adaptive beamforming
ADC: Analogue-to-digital conversion
ASLB: Adaptive sidelobe blanking
BF: Beam forming
CAPS: Constrained adaptive pattern synthesis
CSST: Coherent signal subspace transform
CRB: Cramer-Rao Bound
DSW: Direct subarray weighting
ECCM: Electronic counter-countermeasure
GA: Genetic algorithm
GSLC: Generalized sidelobe canceller
GSP: Gaussian subarray pattern
ISP: Ideal subarray pattern
ISSM: Incoherent signal subspace method
JNR: Jammer-to-noise ratio
LCMV: Linearly constrained minimum variance
LMI: Lean matrix inversion
LMS: Least mean square
LSMI: Load sample matrix inversion
MFPAR: Multifunction phased array radar
MIMO: Multiple-input multiple-output
MLJ: Mainlobe jamming
MLM: Mainlobe maintaining
MOD: Mismatched optimum detector
MOEA: Multiobjective evolutionary algorithm
PAR: Phased array radar
PSL: Peak sidelobe level
SASP: Subarrayed array signal processing
SINR: Signal-to-interference-plus-noise ratio
SLC: Sidelobe canceller
SLJ: Sidelobe jamming
SMI: Sample matrix inverse
SNR: Signal-to-noise ratio
SSP: Subspace projection
STAP: Space-time adaptive processing
ULA: Uniform linear array
UPA: Uniform planar array
WAVES: Weighted average of signal subspace.

Conflict of Interests

The author declares that there is no conflict of interests regarding the publication of this paper.

Acknowledgments

The author would like to thank Dr. Ulrich Nickel of Fraunhofer FKIE, Germany, for his insightful comments and useful discussions. This work has been partially supported by "the Fundamental Research Funds for the Central Universities" (Grant no. HIT.NSRIF.201152), the ASFC (Aeronautical Science Foundation of China, no. 20132077016), and the SAST Foundation (no. SAST201339).

References

[1] U. Nickel, "Array processing for radar: achievements and challenges," *International Journal of Antennas and Propagation*, vol. 2013, Article ID 261230, 21 pages, 2013.

[2] U. R. O. Nickel, "Subarray configurations for digital beamforming with low sidelobes and adaptive interference suppression," in *Proceedings of the IEEE International Radar Conference*, pp. 714–719, IEEE, Alexandria, VA, USA, May 1995.

[3] U. Nickel, "Adaptive beamforming for phased array radars," in *Proceedings of the International Radar Symposium*, pp. 897–906, Munich, Germany, September 1998.

[4] U. Nickel, "Subarray configurations for interference suppression with phased array radar," in *Proceedings of the International Conference on Radar*, pp. 82–86, Paris, France, 1989.

[5] U. Nickel, "Detection with adaptive arrays with irregular digital subarrays," in *Proceedings of the IEEE Radar Conference*, pp. 635–640, Waltham, Mass, USA, April 2007.

[6] U. Nickel, "Super-resolution and jammer suppression with broadband arrays for multi-function radar," in *Applications of Space-Time Adaptive Processing*, R. Klemm, Ed., chapter 16, pp. 543–599, IEE, 2004.

[7] U. Nickel, P. G. Richardson, J. C. Medley, and E. Briemle, "Array signal processing using digital subarrays," in *Proceedings of the IET Conference on Radar Systems*, Edinburgh, UK, October 2007.

[8] W. Bürger and U. Nickel, "Space-time adaptive detection for airborne multifunction radar," in *Proceedings of the IEEE Radar Conference (RADAR '08)*, pp. 1–5, Rome, Italy, May 2008.

[9] R. Klemm and U. Nickel, "Adaptive monopulse with STAP," in *Proceedings of the CIE International Conference on Radar (CIE ICR '06)*, Shanghai, China, October 2006.

[10] U. Nickel, "On the influence of channel errors on array signal processing methods," *International Journal of Electronics and Communication*, vol. 47, no. 4, pp. 209–219, 1993.

[11] U. R. O. Nickel, "Properties of digital beamforming with subarrays," in *Proceedings of the International Conference on Radar (ICR '06)*, Shanghai, China, October 2006.

[12] U. Nickel, "Monopulse estimation with adaptive arrays," *IEE Proceedings, Part F: Radar and Signal Processing*, vol. 140, no. 5, pp. 303–308, 1993.

[13] U. Nickel, "Monopulse estimation with sub-array adaptive arrays and arbitrary sum- and difference beams," *IEE Proceedings—Radar, Sonar and Navigation*, vol. 143, no. 4, pp. 232–238, 1996.

[14] U. Nickel, "Performance of corrected adaptive monopulse estimation," *IEE Proceedings Radar, Sonar and Navigation*, vol. 146, no. 1, pp. 17–24, 1999.

[15] U. Nickel, "Performance analysis of space-time-adaptive monopulse," *Signal Processing*, vol. 84, Special section on new trends and findings in antenna array processing for radar, no. 9, pp. 1561–1579, 2004.

[16] U. Nickel, "Overview of generalized monopulse estimation," *IEEE Aerospace and Electronic Systems Magazine*, vol. 21, no. 6, pp. 27–55, 2006.

[17] U. R. O. Nickel, E. Chaumette, and P. Larzabal, "Statistical performance prediction of generalized monopulse estimation," *IEEE Transactions on Aerospace and Electronic Systems*, vol. 47, no. 1, pp. 381–404, 2011.

[18] E. Chaumette, U. Nickel, and P. Larzabal, "Detection and parameter estimation of extended targets using the generalized monopulse estimator," *IEEE Transactions on Aerospace and Electronic Systems*, vol. 48, no. 4, pp. 3389–3417, 2012.

[19] U. Nickel, "Spotlight MUSIC: super-resolution with subarrays with low calibration effort," *IEE Proceedings: Radar, Sonar and Navigation*, vol. 149, no. 4, pp. 166–173, 2002.

[20] R. Klemm, W. Koch, and U. Nickel, "Ground target tracking with adaptive monopulse radar," in *Proceedings of the European Microwave Association*, vol. 3, pp. 47–56, 2007.

[21] W. R. Blanding, W. Koch, and U. Nickel, "Adaptive phased-array tracking in ECM using negative information," *IEEE Transactions on Aerospace and Electronic Systems*, vol. 45, no. 1, pp. 152–166, 2009.

[22] M. Feldmann and U. Nickel, "Target parameter estimation and tracking with adaptive beamforming," in *Proceedings of the International Radar Symposium (IRS '11)*, pp. 585–590, September 2011.

[23] G. S. Liao, Z. Bao, and Y. H. Zhang, "On clutter DOF for phased array airborne early warning radars," *Journal of Electronics*, vol. 10, no. 4, pp. 307–314, 1993.

[24] W. Blanding, W. Koch, and U. Nickel, "On adaptive phased-array tracking in the presence of main-lobe jammer suppression," in *Signal and Data Processing of Small Targets*, vol. 6236 of *Proceedings of SPIE*, Orlando, Fla, USA, April 2006.

[25] A. Farina, G. Golino, S. Immediata, L. Ortenzi, and L. Timmoneri, "Techniques to design sub-arrays for radar antennas," in *Proceedings of the 12th International Conference on Antennas and Propagation (ICAP '03)*, vol. 1, pp. 17–23, 2003.

[26] A. Farina, "Electronic counter-countermeasures," in *Radar Handbook*, M. I. Skolnik, Ed., chapter 24, McGraw-Hill, 3rd edition, 2008.

[27] A. Farina, G. Golino, and L. Timmoneri, "Maximum likelihood approach to the estimate of target angular co-ordinates under a main beam interference condition," in *Proceedings of the International Conference on Radar*, pp. 834–838, Beijing, China, 2001.

[28] G. Golino, "Improved genetic algorithm for the design of the optimal antenna division in sub-arrays: a multi-objective genetic algorithm," in *Proceedings of the IEEE International Radar Conference*, pp. 629–634, Washington, DC, USA, 2005.

[29] P. Lombardo and D. Pastina, "Pattern control for adaptive antenna processing with overlapped sub-arrays," in *Proceedings of the International Conference on Radar*, pp. 188–193, Adelaide, Australia, September 2003.

[30] P. Lombardo and D. Pastina, "Quiescent pattern control in adaptive antenna processing at sub-array level," in *Proceedings of the IEEE International Symposium on Phased Array Systems and Technology*, pp. 176–181, Boston, Mass, USA, October 2003.

[31] P. Lombardo, R. Cardinali, M. Bucciarelli, D. Pastina, and A. Farina, "Planar thinned arrays: optimization and subarray based adaptive processing," *International Journal of Antennas and Propagation*, vol. 2013, Article ID 206173, 13 pages, 2013.

[32] P. Lombardo, R. Cardinali, D. Pastina, M. Bucciarelli, and A. Farina, "Array optimization and adaptive processing for sub-array based thinned arrays," in *Proceedings of the International Conference on Radar (Radar '08)*, pp. 197–202, Adelaide, Australia, September 2008.

[33] A. Massa, M. Pastorino, and A. Randazzo, "Optimization of the directivity of a monopulse antenna with a subarray weighting by a hybrid differential evolution method," *IEEE Antennas and Wireless Propagation Letters*, vol. 5, no. 1, pp. 155–158, 2006.

[34] S. Caorsi, A. Massa, M. Pastorino, and A. Randazzo, "Optimization of the difference patterns for monopulse antennas by a hybrid real/integer-coded differential evolution method," *IEEE Transactions on Antennas and Propagation*, vol. 53, no. 1, pp. 372–376, 2005.

[35] L. Manica, P. Rocca, and A. Massa, "Design of subarrayed linear and planar array antennas with SLL control based on an excitation matching approach," *IEEE Transactions on Antennas and Propagation*, vol. 57, no. 6, pp. 1684–1691, 2009.

[36] L. Manica, P. Rocca, and A. Massa, "Excitation matching procedure for sub-arrayed monopulse arrays with maximum directivity," *IET Radar, Sonar and Navigation*, vol. 3, no. 1, pp. 42–48, 2009.

[37] Y. F. Kong, C. Zeng, G. S. Liao, and H. H. Tao, "A new reduced-dimension GSC for target tracking and interference suppression," in *Proceedings of the 6th International Conference on Radar (RADAR '11)*, pp. 785–788, Chengdu, China, October 2011.

[38] Z. Y. Xu, Z. Bao, and G. S. Liao, "A method of designing irregular subarray architectures for partially adaptive processing," in *Proceedings of the CIE International Conference on Radar (ICR '96)*, pp. 461–464, Beijing, China, October 1996.

[39] Y. Wang, K. Duan, and W. Xie, "Cross beam STAP for non-stationary clutter suppression in airborne radar," *International Journal of Antennas and Propagation*, vol. 2013, Article ID 276310, 5 pages, 2013.

[40] W.-C. Xie and Y.-L. Wang, "Optimization of subarray partition based on genetic algorithm," in *Proceedings of the 8th International Conference on Signal Processing (ICSP '06)*, Beijing, China, November 2006.

[41] Z. H. Zhang, J. B. Zhu, and Y. L. Wang, "Local degrees of freedom of clutter for airborne space-time adaptive processing radar with subarrays," *IET Radar, Sonar and Navigation*, vol. 6, no. 3, pp. 130–136, 2012.

[42] L. Y. Dai, R. F. Li, and C. Rao, "Combining sum-difference and auxiliary beams for adaptive monopulse in jamming," *Journal of Systems Engineering and Electronics*, vol. 24, no. 3, pp. 372–381, 2013.

[43] R. Klemm, *Principles of Space-Time Adaptive Processing*, IEE, 3rd edition, 2006.

[44] B. D. Carlson, "Covariance matrix estimation errors and diagonal loading in adaptive arrays.," *IEEE Transactions on Aerospace and Electronic Systems*, vol. 24, no. 4, pp. 397–401, 1988.

[45] C. H. Gierull, "Fast and effective method for low-rank interference suppression in presence of channel errors," *Electronics Letters*, vol. 34, no. 6, pp. 518–520, 1998.

[46] H. Hu and X. H. Deng, "An effective ADBF method at subarray level for plane phased array," in *Proceedings of the 8th International Conference on Signal Processing (ICSP '06)*, vol. 4, Beijing, China, November 2006.

[47] H. Hu, E. Liu, and Y. Xiao, "ADBF at subarray level using a generalized sidelobe canceller," in *Proceedings of the 3rd IEEE International Symposium on Microwave, Antenna, Propagation and EMC Technologies for Wireless Communications*, pp. 697–700, Beijing, China, October 2009.

[48] H. Hu and E. X. Liu, "An improved GSLC at subarray level," Submitted.

[49] H. Hu and X. Qu, "An improved subarrayed broadband ABF," Submitted.

[50] H. Hu and X. Qu, "An improved subarrayed fast-time STAP algorithm," Submitted.

[51] D. Wang, H. Hu, and X. Qu, "Space-time adaptive processing method at subarray level for broadband jammer suppression," in *Proceedings of the 2nd IEEE International Conference on Microwave Technology and Computational Electromagnetics (ICMTCE '11)*, pp. 281–284, Beijing, China, May 2011.

[52] H. Hu and W. H. Liu, "A novel analog and digital weighting approach for sum and difference beam of planar array at subarray level," *Chinese Journal of Electronics*, vol. 19, no. 3, pp. 468–472, 2010.

[53] H. Hu, W.-H. Liu, and Q. Wu, "A kind of effective side lobe suppression approach for beam scanning at sub-array level," *Journal of Electronics & Information Technology*, vol. 31, no. 8, pp. 1867–1871, 2009 (Chinese).

[54] A. S. Paine, "Minimum variance monopulse technique for an adaptive phased array radar," *IEE Proceedings—Radar, Sonar and Navigation*, vol. 145, no. 6, pp. 374–380, 1998.

[55] R. L. Fante, "Synthesis of adaptive monopulse patterns," *IEEE Transactions on Antennas and Propagation*, vol. 47, no. 5, pp. 773–774, 1999.

[56] K. B. Yu and D. J. Murrow, "Adaptive digital beamforming for angle estimation in jamming," *IEEE Transactions on Aerospace and Electronic Systems*, vol. 37, no. 2, pp. 508–523, 2001.

[57] H. Hu and H. Zhang, "An improved two-stage processing approach of adaptive monopulse at subarray level," *Acta Electronica Sinica*, vol. 37, no. 9, pp. 1996–2003, 2009 (Chinese).

[58] R. L. Fante, R. M. Davis, and T. P. Guella, "Wideband cancellation of multiple mainbeam jammers," *IEEE Transactions on Antennas and Propagation*, vol. 44, no. 10, pp. 1402–1413, 1996.

[59] C. M. See and A. B. Gershman, "Direction-of-arrival estimation in partly calibrated subarray-based sensor arrays," *IEEE Transactions on Signal Processing*, vol. 52, no. 2, pp. 329–337, 2004.

[60] H. Hu and X. W. Jing, "2-D WSF method at subarray level based on ideal patterns," in *Proceedings of the International Conference on Radar*, pp. 1161–1164, Beijing, China, 2006.

[61] H. Hu and X. W. Jing, "2-D spatial spectrum estimation methods at subarray level for phased array," *Acta Electronica Sinica*, vol. 35, pp. 415–419, 2007 (Chinese).

[62] H. Hu and X. W. Jing, "An improved super-resolution direction finding method at subarray level for coherent sources," in *Proceedings of the CIE International Conference on Radar (ICR '06)*, pp. 525–528, Shanghai, China, October 2006.

[63] H. Hu and X.-W. Jing, "A new super-resolution method at subarray level in planar phased array for coherent source," *Acta Electronica Sinica*, vol. 36, no. 6, pp. 1052–1057, 2008 (Chinese).

[64] H. Hu, X. Liu, and L. J. Liang, "Study on the broadband superresolution direction finding at subarray level," Submitted.

[65] H. Hu, W. C. Qin, and S. Feng, "Optimizing the architecture of planar phased array by improved genetic algorithm," in *Proceedings of the IEEE International Symposium on Microwave, Antenna, Propagation, and EMC Technologies for Wireless Communications (MAPE '07)*, pp. 676–679, Hangzhou, China, August 2007.

[66] A. Hassanien and S. A. Vorobyov, "Phased-MIMO radar: a tradeoff between phased-array and MIMO radars," *IEEE Transactions on Signal Processing*, vol. 58, no. 6, pp. 3137–3151, 2010.

[67] X. P. Luan, H. Hu, and X. Hu, "Analysis on pattern features of MIMO-phased array hybrid radar," Submitted.

[68] D. R. Fuhrmann, J. P. Browning, and M. Rangaswamy, "Signaling strategies for the hybrid MIMO phased-array radar," *IEEE Journal on Selected Topics in Signal Processing*, vol. 4, no. 1, pp. 66–78, 2010.

[69] X. P. Luan, H. Hu, and N. Xiao, "A synthesis algorithm of transmitting beam pattern for MIMO-PAR," Submitted.